UTICAL LABORATORIES

CALIFORNIA INSTITUTE OF TECHNOLOGY

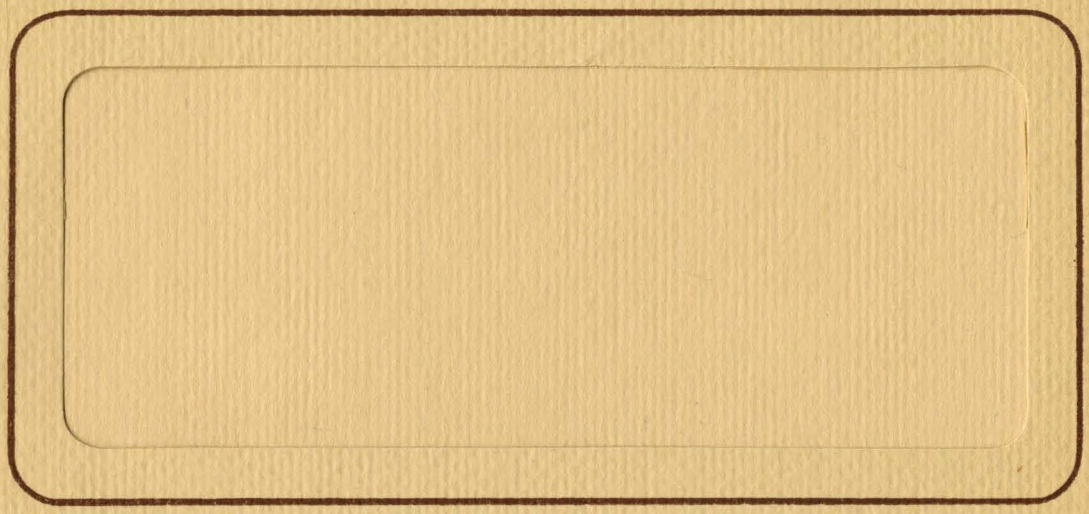

Firestone Flight Sciences Laboratory

Guggenheim Aeronautical Laboratory

Karman Laboratory of Fluid Mechanics and Jet Propulsion

Pasadena

FIRESTONE FLIGHT SCIENCES LABORATORY

GRADUATE AERONAUTICAL LABORATIRIES
CALIFORNIA INSTITUTE OF TECHNOLOGY
Pasadena, California

Propagation of an Initial Density Discontinuity

by

George Bienkowski

HYPERSONIC RESEARCH PROJECT

Memorandum No. 70

May 15, 1964

Contract No. DA-31-124-ARO(D)-33

U. S. Army Research Office and the Advanced Projects Agency

This research is a part of Project DEFENDER sponsored by the Advanced Research Projects Agency.

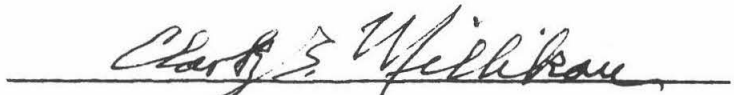

Clark B. Millikan, Director

ACKNOWLEDGEMENTS

The author would like to express his deep appreciation to Professor Lester Lees for suggesting this work and for his continuous guidance during its completion. He would also like to thank Professor Toshi Kubota for his helpful suggestions and stimulating discussions.

Also thanks are due to Mrs. Katherine Cassady who typed this report, and Mrs. Felice Worden who prepared the figures.

A part of this work was carried out under the sponsorship and with the financial support of the U. S. Army Research Office (Durham, North Carolina), and the Advanced Research Projects Agency, Contract No. DA-31-124-ARO(D)-33. This research is a part of Project DEFENDER sponsored by the Advanced Research Projects Agency. The author would also like to acknowledge the help of the National Science Foundation under a Post-Doctoral Fellowship for 1961-1962.

ABSTRACT

The propagation of an initial one-dimensional density discontinuity is studied. The solution for times much shorter than the mean free time between collisions (i. e. collisionless), and the solution for times much longer than the mean free time (i. e. Euler) are functions of the same similarity variable x/t. They differ only in the details of the profiles.

A method for evaluating the first effect of collisions is developed as an expansion in time with coefficients as functions of the similarity variable. The solutions are obtained in detail for both the Krook collision model and the exact collision integral for inverse fifth-power repulsion.

The Krook model is found to agree qualitatively with the "exact" solution except in the region of eventual shock formation for high initial density ratios. In that region the Krook model tends to overestimate the effect of collisions. The first effect of collisions in general alters the free molecular solution in the proper direction towards the Navier-Stokes result. The "first collision" solution appears to be valid up to times of the order of a mean free time between collisions on the high pressure side.

Analysis of the long time solution through the Navier-Stokes equations under the assumption of no interaction between the shock and contact surface indicates that the Euler solution is not relevant until times of the order of 1,000 mean free times. The no-interaction Navier-Stokes solution is valid for times in excess of 50 mean free times. The transition from the "short-time", first collision solution to this "long-time" no-interaction Navier-Stokes solution takes place in a time interval between 1 and 50 collisions per particle. One concludes that the major part of this transition to the "long-time" solution must take place within that part of the Navier-Stokes regime where the shock, contact surface and expansion wave are not distinct but interact with each other.

TABLE OF CONTENTS

LIST OF SYMBOLS

a	collision parameter for inverse fifth power repulsion $b(\lvert\vec{v}-\vec{v}_1\rvert^2/2mK)^{1/4}$
a_o	unperturbed speed of sound (in linearized case)
A_2	collision integral constant evaluated by Maxwell as 1.3682
b	impact parameter in collision process
c_o	most probable speed on the high pressure side $\sqrt{2RT}$
f	velocity distribution function
f_n	n'th order velocity distribution in expansion for f
FN	integral of f over transverse velocities $\iint_{-\infty}^{\infty} f(v_x, v_y, v_z)dv_y dv_z$
FT	integral of f times the sum of squares of the transverse velocities over the transverse velocities $\iint_{-\infty}^{\infty} f(v_x, v_y, v_z)\,(v_y^2, + v_z^2)\,dv_y dv_z$
g_n	time dependent terms in separation of variables solution for f (Appendix)
g_t	transverse component of relative velocity in collision (p. 25)
G_t	transverse component of velocity of center of mass of the colliding particles (p. 25)
h_n	time dependent terms in expansion for collision term J (Appendix)
J	collision term in Boltzmann equation
JN	integral of J (collision term) over the transverse velocities $\iint_{-\infty}^{\infty} J(v_x, v_y, v_z)\,dv_y dv_z$
JT	integral of J times the sum of the squares of the transverse velocities over the transverse velocities $\iint_{-\infty}^{\infty} J(v_x, v_y, v_z)\,(v_y^2 + v_z^2)\,dv_y dv_z$
k	Boltzmann constant
K	proportionality coefficient in inverse fifth power repulsion

K_o, K_1	elliptic function of imaginary argument (Eqs. (4.18) and (4.21))
m	molecular mass
M_s	Mach number of propagating shock
MN, MT	moments of FN and FT defined by Eq. (2.24)
n	number density (ρ/m)
N	similarity variable ($x/c_o t$)
p	pressure (ρRT)
P_{xx}	normal stress in x direction
p_{xx}	difference between total stress and the pressure ($P_{xx} - p$)
q_x	heat flux in x direction
R	gas constant(k/m)
t	time elapsed since the release of imaginary diaphragm
T	temperature
U(x)	unit step function (unity for positive argument, zero otherwise)
$\vec{v}(v_x, v_y, v_z)$	microscopic velocity (and its components)
$\vec{v}_1, \vec{v}_1^{\,1}, \vec{v}^1$	velocities appearing in collision integral
$v(N, \mathscr{R})$	macroscopic velocity in x direction
$v_n(N)$	n'th term in expansion of macroscopic velocity in x direction
x	positive coordinate, also dummy variable of integration
X, Y	transformed variables of integration for obtaining moments (p. 21)
α, β	variables in analysis of fifth power repulsion collision process
δ, ε	variables of integration for obtaining moments $(v_x - N^1)$, $(v_x - N)$ respectively
n_o	collision parameter for inverse fifth power repulsion (p. 30)
$\theta_o, \mathscr{V}$	half angle between asymptotes of collision

K heat conductivity

μ viscosity coefficient

ν collision frequency $(1/\tau_f)$

ρ mass density

σ parameter in fifth power repulsion collision process $(\cos^2\psi)$

τ normalized time (t/τ_{fo})

τ_{fo} initial mean free time between wollisions on high pressure side $(\pi\mu/2\rho_- c_o^2)$

τ_m maximum non dimensional time for validity of first perturbation solution

χ_1 term in Krook model expression for JN_1

Subscripts

+ denotes initial state for $x > 0$

- denotes initial state for $x < 0$

0, 1...n denotes term in solution as expansion in time

e denotes Euler solution

r denotes ratio of initial state in region of $x > 0$ to state in region of $x < 0$

N. S. denotes Navier-Stokes solution

Superscripts

n power of v_x in the expression for moments MN, MT

' generally denotes dummy variable of integration

- denotes average value

LIST OF FIGURES

I. INTRODUCTION

I. 1 Propagation of an initial density discontinuity.

In a number of fluid dynamic problems of current interest solutions are reasonably well established only in the limits of collisionless and collision-dominated flows. In steady external flow problems around bodies, efforts at describing the process of transition from the "free molecular" to the inviscid limit (with possible boundary and shock layers) are hindered by the difficulties in the perturbation away from free-molecular flow. This difficulty is understandable, since collisions always dominate far away from the body, and thus cannot be considered a small perturbation at large distances. In external flow problems one boundary condition has to be applied at infinity, so that any perturbation scheme will necessitate applying boundary conditions in a region where the solution is invalid.

In order to study the effect of collisions, it is therefore more desirable to look at an initial value problem, where the effect of collisions is proportional to the elapsed time expressed in units of the mean free time between collisions. Furthermore to eliminate the uncertainties of gas-solid interface interactions a problem with no solid boundaries can be chosen. One such problem that can yield useful information as to the effects of collision is the sudden release of a gas discontinuity. Conceptually one can imagine two semi-infinite

regions of gas of different thermodynamic states (both in equilibrium) separated by a diaphragm until it is broken at time t = 0. This is just the idealized shock-tube problem. Collisions alter the initial collisionless profile into one containing shock and contact layers which are thin compared to the separation betwe en them. The initial formation of these "discontinuities" is of great fluid dynamic interest.

This particular problem is chosen for the additional reason that both limiting solutions are similarity solutions of the same variable. If a diaphragm is removed at time t = 0, the collisionless and the Euler solutions are both functions of x/t alone. This fact can be of great help in analyzing the effect of collisions. Since the two solutions satisfy the same boundary conditions at plus and minus infinity, they can only vary as to their detailed form in between. The transition solution can be considered in a plane determined by the coordinates x/t and t, where the coordinate t is now a direct measure of the effect of collisions.

The solution of any initial value problem is in principle possible because of the characteristic form of the Boltzmann equation. In practice, however, the calculation of the collision integral along the characteristic requires knowing the value of the distribution function along all the other characteristics, and integration over several variables. In general these integrations cannot be accomplished even with high speed computers. Secondly, certain convergence

difficulties, even with an approximate collision model, make this approach limited in its usefulness to times of the order of a mean free time, as illustrated by Willis (1960). An alternative approach, of course, is to use a moment method. (Lees (1959), Krook (1959)). In this problem, this procedure is equivalent to replacing the infinite set of characteristics V_x = constant in the Boltzmann equation by some finite set which are functions of (x/t) as well as the macroscopic parameters. The large number of simultaneous non-linear differential equations (at least five to retain the independence of the two transport terms) required to obtain a reasonable solution in this problem makes the approach unfruitful.

Another alternative approach would be to use the discrete velocity distribution approximation suggested by Broadwell (1963). In this problem the only mathematical difference from the moment methods would be in changing the characteristics to constants. There is of course some difficulty in the fact that the solution could be strongly dependent on the choice of the discrete velocities for the distribution function.

Monte Carlo methods could in principle also be applied to this problem in a way similar to that used by Haviland and Lavin (1961). The fact that the initial distribution function is known would make the method even more applicable. The fact that two variables are present would greatly increase the numerical difficulties and probably tax even modern high speed computers beyond their capacity.

An alternative approach is to discard the possibility of a direct calculation from collisionless to inviscid flow as unattainable, and concentrate instead on the initial deviations from the two limiting solutions. For long times a Navier-Stokes solution that includes some interaction between the contact surface and the shock would be expected to extend down to about 100 mean free times (based on the high pressure side), and possibly to even shorter times. The first-collision calculation should be valid up to the order of a mean free time. The remaining gap though difficult to bridge should not cause any difficulty, because no unusual new phenomenon is expected to occur there. As an example of the type of information that might be obtained by this approach Figure 1 gives the velocity at the "contact" surface obtained by Goldworthy (1959) by solving the Navier-Stokes equations (without interaction) around the contact surface, and a short time solution obtained in the present work. The two solutions cross at a time equal to 7.5 reference mean free times, or three or four local mean free times, as might be expected. What is important is the fact that the general nature of the solution is determined from these two perturbation solutions, and only quantitative detail could be expected from a more precise calculation of the "transition" regime.

We shall concentrate in this study on the short-time initial effect of collisions. This region is important, because the choice of collision model is most likely to have the greatest

consequences here. Under special initial conditions the exact collision integral required to determine the initial effect of collisions can be sufficiently simplified to make numerical calculation feasible. Thus a real comparison is possible between this "exact" calculation and one based on the Krook model (Bhatnager, Gross and Krook (1954)(which is the one most used in near-free molecular flow analysis).

The general theory of the initial response of gases to the release of a one-dimensional discontinuity is derived in Section II. The calculation of the first order perturbation from the collisionless solution based on the Krook collision model is discussed in Section III. Section IV contains a discussion of this first order perturbation with the exact Boltzmann collision integral for inverse fifth power repulsion. Some remarks about the expected range of validity of these solutions are contained in Section V. The results are presented and some conclusions drawn in Section VI.

II. PERTURBATION FROM COLLISION-FREE SOLUTION

A uniform gas in the half space $x > 0$ has the density ρ_+ and temperature T_+. The half space $x < 0$ is filled with the same gas but at density ρ_- and temperature T_-. The imaginary diaphragm separating the two regions is withdrawn at time $t = 0$. The subsequent motion is governed by the following kinetic equation

$$\frac{\partial f}{\partial t}(v_x, v_y, v_z, x, t) + v_x \frac{\partial f}{\partial x}(v_x, v_y, v_z, x, t) = J(v_x, v_y, v_z, x, t) \qquad (2.1)$$

where f is the distribution function and J is a term representing the net gain per unit time of particles in the velocity space around v_x, v_y, v_z, as a result of collisions.

In general, J is a complicated integral function of f regardless of whether the Boltzmann collision integral or some model term is used. Thus integration along the single characteristic or particle path yields a complicated non-linear integral equation. Presently only limiting solutions for times very short and very long with respect to the mean "free" time are available. The short-time solution is obtained by dropping the collision term and solving the differential equation for f. The long-time solution is obtained by equating the collision term locally to zero everywhere, yielding a Maxwellian distribution function, with parameters determined by defining the mean quantities ρ, u and T.

This long-time solution is the well known idealized shock tube solution and is discussed, for example, by I. I. Glass (1958) and G. N. Patterson (1948). The solution is obtained by matching the velocity and pressure behind a shock propagating into the low pressure region to the velocity and pressure obtained behind the expansion fan propagating into the high pressure region. The density and temperature are discontinuous at the contact front, which moves with the flow velocity. The solution is a function of a single variable x/t, because there can be no separate length or time scale in the problem.

The short time (collisionless) solution is not as well known (first studied by J. B. Keller (1948)), but is very easy to obtain. For an initial value problem such as we are considering, the collisionless Boltzmann equation without body forces has the simple solution

$$f(v_x, v_y, v_z, x, t) = f(v_x, v_y, v_z, x - v_x t, 0) \qquad (2.2)$$

The shift in coordinate $(x - v_x t)$ is an expression of the fact that without collisions or body forces particle paths are straight lines. The relation between f at t and f at zero time expresses the fact that the distribution density is unaltered along particle paths.

If the gas on either side of the diaphragm is initially at rest and at equilibrium, it seems reasonable to specify the initial distribution function as a different Maxwellian for $x > 0$ and $x < 0$ i. e.

$$f(v_x, v_y, v_z, x, 0) = n_{\pm} \left(\frac{m}{2\pi k T_{\pm}} \right)^{3/2} \exp\left(\frac{-m(v_x^2 + v_y^2 + v_z^2)}{2kT_{\pm}} \right) \quad \text{for } x \gtrless 0 \qquad (2.3)$$

where k is Boltzmann constant, m the molecular mass, and n is ρ/m the number density. For these initial conditions integration to obtain the moments can be done immediately. A lack of a characteristic time or length scale again insures that the solutions are functions of the variable x/t alone. The physically significant moments are:

$$\rho_o\left(\frac{x}{t}\right) = \frac{\rho_-}{2}\left[1 - \operatorname{erf}\left(\frac{x}{t\sqrt{2RT_-}}\right)\right] + \frac{\rho_+}{2}\left[1 + \operatorname{erf}\left(\frac{x}{t\sqrt{2RT_+}}\right)\right] \qquad (2.4)$$

$$\rho_o v_o\left(\frac{x}{t}\right) = \frac{\rho_-\sqrt{2RT_-}}{2\sqrt{\pi}} \exp\left(-\frac{x^2}{2RT_- t^2}\right) - \frac{\rho_+\sqrt{2RT_+}}{2\sqrt{\pi}} \exp\left(-\frac{x^2}{2RT_+ t^2}\right) \qquad (2.5)$$

$$p_o\left(\frac{x}{t}\right) = \frac{\rho_- RT_-}{2}\left(1 - \operatorname{erf}\left(\frac{x}{\sqrt{2RT_-}t}\right)\right) + \frac{\rho_+ RT_+}{2}\left(1 + \operatorname{erf}\left(\frac{x}{\sqrt{2RT_+}t}\right)\right)$$

$$+ \frac{\rho_o v_o}{3}\left(\frac{x}{t} - v_o\right) \qquad (2.6)$$

$$p_{xx_o} = (P_{xx} - p)_o = \frac{2}{3}\rho_o v_o\left(\frac{x}{t} - v_o\right) \qquad (2.7)$$

$$q_{xo} = \frac{\rho_o v_o}{2}\left(\frac{x}{t} - 2v_o\right)\left(\frac{x}{t} - v_o\right) - \frac{5}{2}v_o\left[p_o - \frac{\rho_o v_o}{3}\left(\frac{x}{t} - v_o\right)\right]$$

$$+ \rho_- RT_- \frac{\sqrt{2RT_-}}{\sqrt{\pi}} \exp\left(\frac{-x^2}{2RT_- t^2}\right) - \rho_+ RT_+ \frac{\sqrt{2RT_+}}{\sqrt{\pi}} \exp\left(\frac{-x^2}{2RT_+ t^2}\right) \qquad (2.8)$$

where R is k/m, the gas constant.

Figure 2 is a comparison of the Euler and collisionless solutions for the case of uniform initial temperature. The velocity and density profiles are shown for three initial density ratios $\rho_+/\rho_- = 0.298,\ 0.0201,\ 0.375 \times 10^{-3}$, which correspond to shock Mach numbers in the Euler limit of $M_s = 1.27,\ 2.00$ and 3.00, respectively. The similarity between the Euler and collisionless solutions is remarkable. The "collisionless" velocity profile is much steeper on the low density side than on the high density side, although not in as pronounced a way as the Euler solution. The "collisionless" density profile looks in many respects like the best mean smooth curve through the discontinuous Euler profile. These similarities suggest that the broad aspects of the solution for this initial value problem are determined by the kinematics rather than the details of the interaction or non-interaction between particles. Conservation of mass and momentum guarantee that the integrals under the curves have to be identical for the two solutions. The additional fact that the mean molecular speed and the speed of sound are of the same order guarantees that the (x/t) scale for both solutions is similar.

The proper solution for large time is really the Navier-Stokes solution with a contact surface growing as $\sqrt{t}$ and a constant thickness shock wave. In the (x/t) variable of (Figure 2) the discontinuities of the Euler solution have to be modified by "boundary

layers" of thicknesses of order $1/\sqrt{t}$ and $1/t$ for the contact surface and the shock wave respectively. Thus, for any finite time the smoothing of the discontinuities would make the qualitative similarity between the "short" and "long" time solutions more pronounced. The effect of collisions is limited in this problem primarily to local steepening of gradients (in the x/t variable) in the vicinity of the contact surface and shock wave.

The fact that both asymptotic solutions (for $t \to 0$ and $t \to \infty$) are functions of (x/t) only suggests the transformation to a new coordinate system proportional to x/t, and t, where now t will be a direct measure of the effect of collisions. We define new variables $N = x/c_o t$ and $\tau = t/\tau_{f_o}$ where c_o is $\sqrt{2RT_-}$ and τ_{f_o} is the reciprocal of the collision frequency at $x \to -\infty$. By non-dimensionalizing the other variables as $\bar{f} = (m)c_o^3/\rho_- \cdot f$ and $\bar{J} = \rho_- \tau_{f_o}/mc_o^3 \cdot J$ and $\bar{v}_x, \bar{v}_y, \bar{v}_z = v_x/c_o, v_y/c_o, v_z/c_o$ respectively, we obtain a new form of the Boltzmann equation

$$\tau \frac{\partial f}{\partial \tau}(v_x, v_y, v_z, N, \tau) + (v_x - N) \frac{\partial f}{\partial N}(v_x, v_y, v_z, N, \tau) = \tau J(v_x, v_y, v_z, N, \tau) \qquad (2.9)$$

where the bars have been dropped for ease of notation.

The initial conditions in the new variables can be stated as

$$f(v_x, v_y, v_z,\ N \to -\infty,\ 0) = \frac{\exp\left(-(v_x^2 + v_y^2 + v_z^2)\right)}{(\pi)^{3/2}}$$

$$f(v_x, v_y, v_z,\ N \to \infty,\ 0) = \frac{\rho_r \exp\left(-\dfrac{v_x^2 + v_y^2 + v_z^2}{T_r}\right)}{(\pi T_r)^{3/2}} \qquad (2.10)$$

where $\rho_r = \rho_+/\rho_-$ and $T_r = T_+/T_-$.

This equation can be integrated by the method of characteristics to yield

$$f(v_x, v_y, v_z, N, \gamma) = (v_x - N)\gamma \int_{\pm\infty}^{N} \frac{J(v_x, v_y, v_z, N^1, \frac{v_x - N}{v_x - N^1}\gamma)dN^1}{(v_x - N^1)^2}$$

$$+ f(v_x, v_y, v_z,\ N \to \pm\infty,\ 0) \qquad \text{for } (N - v_x) \gtrless 0 \qquad (2.11)$$

If J was just a given function Eq. (2.11) would of course be an exact solution. Since, however, J is itself dependent on an integral of f this result is an integral equation. When $\gamma \to 0$ there exists the possibility of a perturbation type of solution obtained by evaluating J from f_o (the collisionless solution), and thus obtaining f_1 linear in γ, etc. This procedure yields solutions in the form of a power series in γ with the coefficient of γ^n being determined by integrals of J_{n-1}, which in turn is a

function of all the lower coefficients of the f expansion up to $\mathcal{V}^{n-1}$, * i.e.,

$$f(v_x, v_y, v_z, N, \mathcal{V}) = \sum_{n=0}^{\infty} f_n(v_x, v_y, v_z, N)\mathcal{V}^n \tag{2.12}$$

and $$J(v_x, v_y, v_z, N, \mathcal{V}) = \sum_{n=0}^{\infty} J_n(v_x, v_y, v_z, N)\mathcal{V}^n \tag{2.13}$$

where $$f_n(v_x, v_y, v_z, N) = (v_x - N)^n \int_{\pm\infty}^{N} \frac{J_{n-1}(v_x, v_y, v_z, N^1)dN^1}{(v_x - N^1)^{n+1}}$$

$$n \geqslant 1 \quad \text{for } (N - v_x) \gtrless 0 \tag{2.14}$$

and $$f_o(v_x, v_y, v_z, N) = \frac{e^{-(v_x^2 + v_y^2 + v_z^2)}}{\pi^{3/2}} \qquad v_x > N \tag{2.15}$$

$$\rho_r \frac{e^{-(v_x^2 + v_y^2 + v_z^2)/T_r}}{(\pi T_r)^{3/2}} \qquad v_x < N$$

The same results could have been obtained from the differential equation (Eq. 2.9) directly by assuming that f can be expanded in a Taylor series in $\mathcal{V}$.

---

* If the equation had been integrated along the characteristics by splitting the collision term into a loss and a gain term and then keeping the loss term $-\nu f$ on the left as done by Willis (1958) the integral equation would of course have a different form. It can, however, be easily verified that at least the first order term obtained by evaluating the gain term on the basis of the collisionless solution can in this problem be expanded in $\mathcal{V}$ to yield the term linear in $\mathcal{V}$ identical to that obtained by our method.

Setting aside for the present the questions of validity we look at the solution for $f_1(v_x, v_y, v_z, N)$ as the evaluation of the slope $(\partial f/\partial \tau)\tau \longrightarrow 0$. This coefficient represents the initial effect of collisions. Since one purpose of this paper is to study the validity of the "Krook's" collision model, the "nearly collision free" region is of the greatest importance, because the limitations of the model are likely to be most stringent there. This first order perturbation away from the collisionless solution coupled with some approximate Navier-Stokes solution for large times should go a long way towards determining the transition from the collisionless to the collision-dominated regime in this initial value problem.

We are interested mainly in the moments of f_1 and not f_1 itself. These moments are non-singular if J_o is either analytic or has an integrable singularity at $v_x = N$. Before proceeding to prove this statement we first express all the physically meaningful moments in a more convenient form. If we confine ourselves to moments no higher than the heat flux, we notice that in this one-dimensional problem integrations over the transverse velocities v_y and v_z can be carried out in advance, Since only 1 and $(v_y^2 + v_z)^2$ enter into the integrations over v_y and v_z we can define new functions

$$FN_n = \int_{-\infty}^{\infty}\int f_n dv_y dv_z$$

and

$$FT_n = \int_{-\infty}^{\infty}\int f_n(v_y^2 + v_z^2)\, dv_y dv_z \qquad (2.16)$$

as well as JN and JT similarly defined.

Now FN_1 is related to JN_o, while FT_1 is related to JT_o only. The perturbation moments can in turn be defined in terms of single integrals of FN_1 and FT_1 over v_x. Suppose the physically meaningful variables are considered as expansions analogous to the expansion of the distribution function, as follows:

density $\rho = \rho_o(N) + \rho_1(N)\wp + \ldots$ Temperature $T = T_o(N) + T_1(N)\wp \ldots$

velocity $v = V_o(N) + v_1(N)\wp \ldots$ stress $p_{xx} = p_{xx_o}(N) + p_{xx_1}(N)\wp \ldots$

pressure $p = p_o(N) + p_1(N)\wp \ldots$ heat flux $q_x = q_{x_o}(N) + q_{x_1}(N)\wp \ldots$

(2.17)

where zeroth order quantities are the collisionless solutions determined by equations 2.4 through 2.8, and non-dimensionalized. The expressions for the first order quantities are:

$$\rho_1(N) = MN_1^o \qquad (2.18)$$

$$v_1(N) = (MN_1^1 - \rho_1 v_o)/\rho_o \qquad (2.19)$$

$$p_1(N) = 2(MN_1^2 - v_o\rho_o + MN_1^1 v_o) + MT_1^o/3 \qquad (2.20)$$

$$T_1(N) = (p_1 - T_o\rho_1)/\rho_o \qquad (2.21)$$

$$p_{xx_1}(N) = 2(p_1 - MT_2^o) \qquad (2.22)$$

$$q_{x_1}(N) = MN_1^3 + MT_1^1 - v_o(3(MN_1^2 - v_o MN_1^1) + MT_1^o - \rho_1 v_o^2) - \frac{v_1}{4}(2\rho_o + 9q_{x_o}) \tag{2.23}$$

where $$MN_1^n = \int_{-\infty}^{\infty} v_x^n FN_1 dv_x$$

and $$MT_1^n = \int_{-\infty}^{\infty} v_x^n FT_1 dv_x \tag{2.24}$$

Since ρ_o does not go to zero anywhere and all the zeroth order variables have no singularities the only singularities of the first order variables arise from the MN_1^n's and the MT_1^n's. These quantities can be related to the JN_o and JT_o as follows.

$$MN_1^n = \int_N^{\infty} v_x^n (v_x - N) \int_{-\infty}^{N} \frac{JN_o(v_x, N^1)}{(v_x - N^1)^2} dN^1 dv_x + \int_{-\infty}^{N} v_x^n (v_x - N) \int_{\infty}^{N} \frac{JN_o(v_x, N^1)}{(v_x - N^1)^2} dN^1 dv_x \tag{2.25}$$

with a similar relation for MT_1^n. By defining new variables $\mathcal{E} = v_x - N$ and $\delta = v_x - N^1$ and interchanging orders of integration we obtain

$$MN_1^n = \int_{-\infty}^{\infty} \int_0^{\delta} (N + \mathcal{E})^n \frac{\mathcal{E}}{\delta^2} JN_o(N + \mathcal{E}, N + \mathcal{E} - \delta) d\mathcal{E} d\delta \tag{2.26}$$

again with a similar relation for MT_1^n. In this form it is apparent that as long as the singularity of $JN_o(v_x, N)$ is integrable at $v_x = N$ the MN_1^n for any positive n will have no singularity in N.

We are now ready to look at the details of the solution in both the Krook and the exact collision integral cases.

III. KROOK COLLISION MODEL

In order to avoid the complexities of the collision integral it is often replaced by a model term first suggested by Bhatnager, Gross and Krook (1954). This model can best be considered as an ad-hoc assumption where certain assumed free parameters in the collision term are related to macroscopic properties by requiring the conservation of mass, momentum and energy as well as the best fit to the approach to equilibrium results. The collision term is usually written as

$$J = c\nu(f_{eq} - f) \tag{3.1}$$

where c is a constant, ν is a local collision frequency (independent of particle velocity) and f_{eq} is the local Maxwellian distribution function with local density, velocity and temperature as parameters. The model can be justified as plausible because it has several properties that are identical to the exact collision integral. The loss term $-c\nu f$ has the correct form, and for the case of inverse fifth power repulsion is identical to the exact term (because ν can then be assumed as independent of particle velocities). The gain function $c\nu f_{eq}$ has the correct form to guarantee the three conservation laws for the collision process, as well as giving the correct "relaxation to equilibrium" type of behaviour with f going to f_{eq} when collisions dominate. The fact that only one constant

c is present means that only a single collision "time" (relaxation constant) can be defined. This means that c can be chosen to match correctly one of the transport properties such as viscosity, or conductivity but not both. The model therefore inherently fixes the value of the Prandtl number in the continuum limit.

In our notation the model becomes:

$$J(v_x, v_y, v_z, N, \tau) = c\,\tau_f\,\nu(N,\tau)\left[\frac{\rho(N,\tau)}{(2\pi RT(N,\tau))^{3/2}}\exp\left(\frac{-((v_x - v(N,\tau))^2 + v_y^2 + v_z^2)}{2RT(N,\tau)}\right) - f(v_x, v_y, v_z, N, \tau)\right] \qquad (3.2)$$

One should not, however, be misled by the relative simplicity of the form to assume that the solution can now be obtained directly. The first term in the bracket is not a known function but depends on f through the parameters ρ, v, T which are integrals of f over velocity space. In a perturbation scheme, such as suggested here, ρ, v, T from a lower order solution are used. The fact that the collision term is only algebraically related to these quantities makes this much simpler than the exact collision integral.

The perturbation from the collisionless solution, f_1, can then be evaluated in terms of the integral over functions involving only the density, ρ_o, velocity, v_o, and temperature T_o, based on the collisionless solution. The quantity J_o is a function which has a discontinuity at $v_x = N$ (contained in f_o), but J_o is well defined and analytic everywhere else in the v_x, N plane. From the form of the expression for f_1 (Eq. 2.14) it is apparent that there is a possibility of singular behaviour at $v_x = N$. For J_o determined by the Krook model, f_1 in the vicinity of $v_x = N$ can be determined by successive partial integrations for either $v_x > N$ or $v_x < N$ without ever having any difficulty with the discontinuity at $v_x = N$. For either $v_x > N$ or $v_x < N$ the function f_1 has the form

$$f_1(v_x, v_y, v_z, N) = J_o(v_x, v_y, v_z, N) - (v_x - N)\frac{dJ_o}{dN}(v_x, v_y, v_z, N) \ln(|v_x - N|) + \ldots \qquad (3.3)$$

near $v_x = N$. Thus f_1 is finite though discontinuous at $v_x = N$ because of the discontinuity in J_o. The approach from either side to $v_x = N$ is $(v_x - N) \ln(|v_x - N|)$; thus the first derivative is logarithmically infinite. Figure 3 is a typical three dimensional profile for FN_1 (defined by Eq. 2.16), for an initial density discontinuity. Any integral over v_x is quite insensitive to the detailed behaviour of FN_1 at $v_x = N$. Not only does that region contribute only a portion of the total integral but the contributions from the two sides of $v_x = N$ tend to cancel each other.

The moments can be calculated directly from equations (2.18) to (2.23) with JN_o and JT_o expressed as follows

$$JN_o = c\rho_o(N)\left(\frac{\rho_o(N)}{(\pi T_o(N))^{1/2}} \exp\left(-\frac{(v_x - v_o(N))^2}{T_o(N)}\right) - f_o(v_x, N)\right) \quad (3.4)$$

and

$$JT_o = c\rho_o(N)\left(\frac{\rho_o(N)T_o(N)^{1/2}}{\pi} \exp\left(-\frac{(v_x - v_o(N))^2}{T_o(N)}\right) - f_o(v_x, N)\right)$$

ν_o has to be chosen proportional to ρ_o to facilitate later comparison to the results obtained by use of the exact collision integral for Maxwellian particles. The value of the constant is chosen as $c = \pi/4$ in order to make the fourth moment equation (for the stress) take the correct form for Maxwellian molecules where $\nu = \pi/4\ \mu/p$ is taken as a definition of collision frequency. This choice however, forces the coefficient of the collision term in the heat flux moment equation to be incorrect by the factor 3/2. Because of the non-singular behaviour of JN_o and JT_o the moments will all be non-singular and well behaved.

The numerical work of calculating the moments was carried out for the case of an initial density discontinuity but equal initial temperature on both sides of the diaphragm, even though this restriction is not an essential one. However in the "exact" case this choice of initial conditions introduces great simplification. Since the basic features of the solutions are not altered in the limits $\nu \to 0, \nu \to \infty$, the assumption was not considered serious.

The numerical solution was carried out in a straight forward manner. Functions JN_o and JT_o were defined in analytical form in terms of the initial density discontinuity by combining equations 3.4 with 2.4 and 2.8. Equation 2.26 was put in a more convenient form for numerical integration by changing to the variables $X = \xi/\delta, Y = |\delta|$ and the resulting equation for any moment to

$$MN_1^n = \int_0^\infty \int_0^1 X\Big[(N+XY)^n JN_o(N+XY, N-Y(1-X)) + (N-XY)^n JN_o(N-XY, N+Y(1-X))\Big] dXdY \qquad (3.5)$$

with a similar relation for MT_1^n. The physical variables were evaluated through equation 2.18 to 2.23.

The numerical integration was carried out by quadratures. The Legendre-Gauss quadrature (Lowan, Davids and Levenson (1942)) was chosen for X while a combination Legendre-Gauss and a modified Laguerre (National Bureau of Standards (1954)) quadrature(in Y^2) was used for the Y integration, in order to obtain the correct representation near infinity, while still evaluating the region around Y = 0 properly. Accuracy was checked by changing the orders of the quadratures and by evaluating some trial cases by direct Simpson's rule integration. The quadrature

results were found to be accurate within about one percent with much shorter computing times than Simpson's rule. The numerical results are given in figures 8 through 14 together with the results obtained by using the "exact" collision integral for Maxwellian molecules.

IV. "EXACT" COLLISION INTEGRAL

In the "exact" form of the Boltzmann equation the collision term has the general form

$$J(\vec{v},\ \vec{r},\ t) = \iiint \left\{ f(\vec{v}^{1},\ \vec{r},\ t)\, f(\vec{v}_1^{\,1},\ \vec{r},\ t) - f(\vec{v},\ \vec{r},\ t)\, f(\vec{v}_1,\ \vec{r},\ t) \right\} \cdot \left| \vec{v} - \vec{v}_1 \right| \ b\,db\,d\varepsilon\, d^3\vec{v}_1 \qquad (4.1)$$

where b and ε are the parameters of collision, $\vec{v}$, $\vec{v}_1$ are the velocities of the particles before collision and $\vec{v}^{1}$, $\vec{v}_1^{\,1}$, are the velocities after collision. To calculate J_o in the present expansion appears straight forward since f_o is known. However, this calculation is not in general feasible, since J_o itself is a five-fold integral, while the perturbation moments require three more velocity integrations and one space integration over N^1.

The particular choice of initial conditions as an initial density discontinuity with the same temperature on both sides yields such a simple form for f_o, that regardless of the particle interaction model, J_o can be evaluated by two numerical integrations, while the moments require only two additional numerical integrations (as in the Krook model). By choosing Maxwellian molecules (fifth power repulsion particle interaction) another integration in the term linear in $(1 - \rho_r)$ can be evaluated analytically.

In our notation f_o takes the form:

$$f_o(v_x, v_y, v_z, N) = \left[1 - (1 - \rho_r)\, U(N - v_x)\right] \frac{e^{-(v_x^2 + v_y^2 + v_z^2)}}{\pi^{3/2}} \qquad (4.2)$$

where $U(N - v_x)$ is the unit function (zero for negative argument and unity for positive argument). By substituting this f_o into the expression for JN_o, with the proper normalizations to correspond to our non-dimensional coordinates we obtain the expression (after conservation of energy $\vec{v}^2 + \vec{v}_1^2 = \vec{v}'^2 + \vec{v}_1'^2$ has been used)

$$JN_o(v_x, v_y, v_z, N) =$$

$$\left(\frac{\rho_- \, \gamma_f}{m}\right) \int_{-\infty}^{\infty}\int_{-\infty}^{\infty}\int_{-\infty}^{\infty}\int_{0}^{2\pi}\int_{0}^{\infty} \left\{ \frac{2(1-\rho_r)}{2}\left[U(N - v_x) + U(N - v_{x_1}) - U(N - v_x') - U(N - v_{x_1}')\right] \right.$$

$$\left. + 4\left(\frac{1-\rho_r}{2}\right)^2 \left[U(N - v_x')\, U(N - v_{x_1}') - U(N - v_x)\, U(N - v_{x_1})\right] \right\} \frac{\exp(-(v^2 + v_1^2))}{\pi^3} \cdot$$

$$\left(\sqrt{(v_x - v_{x_1})^2 + (v_y - v_{y_1})^2 + (v_z - v_{z_1})^2}\right) b\, db\, d\varepsilon\, dv_{y_1}\, dv_{z_1}\, dv_{x_1}\, dv_y\, dv_z \qquad (4.3)$$

JT_o is identical except for an additional factor $(v_y^2 + v_z^2)$ multiplying the integrand.

Regardless of the actual numerical value of the integral its dependence on the initial density ratio is only quadratic, whereas the Krook model depends on $(1 - \rho_r)$ in a much more

complicated way. An expansion of the Krook model in $(1 - \rho_r)$ would necessarily yield higher order terms. One would suspect therefore that the Krook model cannot be an equally valid representation for the collision process for the entire range of initial density ratios. Furthermore from this form as well as physical consideration in the justification of the Krook model its accuracy would be expected to improve as $(1 - \rho_r) \longrightarrow 0$.

Since the two terms in Equation 4.3 can be evaluated separately we divide the collision integral into JN_{ol} and JN_{os} (as well as JT_{ol} and JT_{os}), which are coefficients of the $(1 - \rho_r)/2$ and $((1 - \rho_r)/2)^2$ terms, respectively. We now indicate the method of evaluating the collision integral by following in detail the evaluation of a typical term

$$\int_{-\infty}^{\infty}\int_{0}^{2\pi}\int_{0}^{\infty} U(N - v_x^1)\, \frac{e^{-(v_x^2 + v_y^2 + v_z^2 + v_{x_1}^2 + v_{y_1}^2 + v_{z_1}^2)}}{\pi^3} \cdot \sqrt{(v_x - v_{x_1})^2 + (v_y - v_{y_1})^2 + (v_z - v_{z_1})^2}\; b\,db\,d\varepsilon\, dv_{y_1} dv_{z_1} dv_{x_1} dv_y dv_z \quad (4.4)$$

Three integrations can be carried out immediately by the change of variables

$$v_y + v_{y_1} = G_t \sin\theta \qquad v_y - v_{y_1} = g_t \sin\varphi$$

$$v_z + v_{z_1} = G_t \cos\theta \qquad v_z - v_{z_1} = g_t \cos\varphi \quad (4.5)$$

and yield

$$\int_{-\infty}^{\infty}\int_{0}^{\infty}\int_{0}^{2\pi}\int_{0}^{\infty} U(N - v_x^1)\,\frac{e}{\pi}\,\frac{-(v_x^2 + v_{x_1}^2 + \frac{g_t^2}{2})}{\sqrt{(v_x - v_{x_1})^2 + g_t^2}} \cdot bdbd\ g_t dg_t dv_{x_1} \tag{4.6}$$

where from Jeans (1954), Chapter VIII

$$v_x^1 = v_x + (v_{x_1} - v_x)\cos^2\Psi + g_t \sin\Psi \cos\Psi \cos\varepsilon$$

and Ψ is the half angle of the deflection during a collision. Its dependence on b, $(v_x - v_{x_1})$ and g_t determines the collision model. Two choices offer further simplification. In the case of hard sphere collisions the independence of b and $g = \sqrt{(v_x - v_{x_1})^2 + g_t^2}$ allows analytical evaluation of the integrations with respect to b and ε. In the case of Maxwellian molecules replacement of gbdb by $\sqrt{2mK}$ ada, where $a = b\,(g^2/2mK)^{1/4}$, allows the analytical evaluation of all but the integration with respect to a, which has to be done numerically because of the implicit relation between Ψ and a. We shall confine ourselves now to Maxwellian molecules.

The typical integral to be solved therefore becomes

$$\int_{-\infty}^{\infty}\int_{0}^{\infty}\int_{0}^{\infty}\int_{-1}^{+1} U(N - v_x + (v_x - v_{x_1})\sigma - g_t\sqrt{\sigma(1-\sigma)}\xi)\,\exp(-(v_x^2 + v_{x_1}^2 + \frac{g_t^2}{2}))\cdot\frac{d\xi}{\sqrt{1-\xi^2}}\,\frac{da^2(\sigma)}{\pi}\,g_t dg_t dv_{x_1} \tag{4.7}$$

where $\xi = \cos \mathcal{E}$ and $\sigma = \cos^2 \Psi$ substitutions have been made. This integral can be transformed to the following form

$$\int_0^\infty \int_{-\infty}^{N} \int_{-\infty}^{\infty} \int_0^\infty U\left(g_t \sqrt{\sigma(1-\sigma)} - \left|\tilde{N} - v_x + (v_x - v_{x_1})\,\sigma\right|\right) \cdot \frac{e^{-\left(v_x^2 + v_{x_1} + \frac{g_t^2}{2}\right)}}{\pi \sqrt{g_t^2\,\sigma\,(1-\sigma) - (\tilde{N} - v_x + (v_x - v_{x_1})\,\sigma)^2}} \, g_t dg_t dv_{x_1} d\tilde{N} da^2 \tag{4.8}$$

by differentiating the integrand with respect to N and then integrating back after integration over ξ, g_t, and v_x, has been accomplished. Alternatively the integration over ξ can be considered as being transformed to the integration over $\tilde{N}$ with a subsequent change in the orders of integration*. The g_t integration can be carried out by shifting to a new variable $x = g_t^2/2 - (\tilde{N} - v_x + (v_x - v_{x_1})\,\sigma)^2/\sigma(1-\sigma)$ which result in the form

$$\int_0^\infty \int_{-\infty}^{N} \int_{-\infty}^{\infty} \frac{e^{-\left(v_x^2 + v_{x_1}^2 + \frac{(\tilde{N} - v_x + (v_x - v_{x_1})\sigma)^2}{\sigma(1-\sigma)}\right)}}{\sqrt{\sigma(1-\sigma)}} \frac{dv_{x_1}}{\pi} d\tilde{N} da^2(\sigma) \int_0^\infty e^{-x} \frac{dx}{\sqrt{x}} \tag{4.9}$$

---

* Integration of quantity (4.7) can be accomplished by first differentiating with respect to N, which yields a δ function from the unit function. The integration over ξ is now facilitated, while the original quantity is regained by later integration over N. Alternatively (if δ functions are to be avoided) the transformation to the form in (4.8) can be accomplished by a purely formal transformation from ξ to $\tilde{N}$ in such a way that integration over ξ from -1 to +1 yields an answer identical to integration over N from $-\infty$ to N, followed by a subsequent change of the order of integrations. The results of the two methods are identical.

Subsequent completion of the square in the exponent for $v_{x_1'}$ integration over v_{x_1}, and a completion of the square in $\tilde{N}$ followed by integration yields

$$e^{-v_x^2} \frac{\sqrt{\pi}}{2} \int_0^\infty \left(1 + \operatorname{erf}\left(\frac{N - v_x(1-\sigma)}{\sqrt{\sigma(2-\sigma)}}\right)\right) da^2(\sigma) \qquad (4.10)$$

Evaluating the other terms in a similar manner, with Maxwell's definition of collision frequency as $\nu = 4/\pi \cdot p/\mu$ where μ is $kT/(3/2\ A_2\sqrt{2mK})$ and $A_2 = 1.3682$, the linear terms in the collision integral become:

$$JN_{ol} = 0.4775\, e^{-v_x^2} \sqrt{2}$$

$$\cdot \int_0^\infty \left[\text{sign}\,(N - v_x) + \operatorname{erf}(N) - \operatorname{erf}\left(\frac{N - v_x\sigma}{\sqrt{1-\sigma^2}}\right) - \operatorname{erf}\left(\frac{N - v_x(1-\sigma)}{\sqrt{\sigma(2-\sigma)}}\right)\right] d(a^2(\sigma)) \qquad (4.11)$$

and

$$JT_{ol} = JN_{ol} + \frac{0.4775}{\sqrt{\pi}}\, e^{-v_x^2} \sqrt{2}$$

$$\cdot \int_0^\infty \left[\frac{(N - v_x\sigma) \exp\left(\frac{-(N - v_x\sigma)^2}{(1-\sigma^2)}\right)}{\sqrt{1-\sigma^2}} \left(\frac{\sigma}{1+\sigma}\right) + \frac{N - v_x(1-\sigma)}{\sqrt{\sigma(2-\sigma)}} \right.$$

$$\left. \exp\left(-\frac{(N - v_x(1-\sigma))^2}{\sigma(2-\sigma)}\right) \left(\frac{1-\sigma}{2-\sigma}\right)\right] da^2(\sigma) \qquad (4.12)$$

The non-linear terms are obtained by similar methods, although analytical integrations cannot be carried out as far as in the linear case. The relations become

$$JN_{os} = 0.4755\sqrt{2}\; e^{-v_x^2}$$

$$\cdot\int_0^{\infty}\left[\frac{2}{\sqrt{\pi}}\int_{-\infty}^{2N-v_x} e^{-v_{x_1}^2}\left\{\operatorname{erf}\left(\frac{N-v_x\sigma-v_{x_1}(1-\sigma)}{\sqrt{2\sigma(1-\sigma)}}\right)+\operatorname{erf}\left(\frac{N-v_x(1-\sigma)-v_{x_1}\sigma}{\sqrt{2\sigma(1-\sigma)}}\right)\right\}dv_{x_1}\right.$$

$$\left.-2U(N-v_x)\,(1+\operatorname{erf}(N))\right]\,da^2(\sigma) \qquad (4.13)$$

and

$$JT_{os} = JN_{os} - \frac{0.4755\sqrt{2}}{\sqrt{\pi}}\; e^{-v_x^2}$$

$$\int_0^{\infty}\left[\left(\frac{\sigma}{1+\sigma}\right)\exp\left(-\frac{(N-v_x\sigma)^2}{1-\sigma^2}\right)\left\{\left(\frac{N-v_x\sigma}{\sqrt{1-\sigma^2}}\right)\left(1+\operatorname{erf}\left(\frac{(1+2\sigma)N-v_x}{\sqrt{2\sigma(1+\sigma)}}\right)\right)\right.\right.$$

$$\left.+0.2821\sqrt{\frac{2(1-\sigma)}{\sigma}}\exp\left(-\frac{((1+2\sigma)N-v_x)^2}{2\sigma(1+\sigma)}\right)\right\}+\left(\frac{1-\sigma}{2-\sigma}\right)\exp\left(-\frac{(N-v_x(1-\sigma))^2}{\sigma(2-\sigma)}\right)$$

$$\left.\left\{\left(\frac{N-v_x(1-\sigma)}{\sqrt{\sigma(2-\sigma)}}\right)\left(1+\operatorname{erf}\left(\frac{(3-2\sigma)N-v_x}{\sqrt{2(1-\sigma)(2-\sigma)}}\right)\right)+0.2821\sqrt{\frac{2\sigma}{1-\sigma}}\exp\left(-\frac{((3-2\sigma)N-v_x)^2}{2(1-\sigma)(2-\sigma)}\right)\right\}\right]da^2(\sigma)$$

(4.14)

The integration over a (σ) can be carried out by solving for a (σ) as a function of σ through the calculation of the collision process for inverse fifth power repulsion. Following the notation of Jeans we can obtain a as a function of σ as follows

$$\sigma = \cos^2 \theta_o$$

$$\theta_o = \eta_o \int_0^1 \frac{dx}{\sqrt{1 - x^2}\sqrt{1 + (1 - \eta_o^2) x^2}} = \eta_o K_o(\eta_o^2 - 1) \qquad (4.15)$$

where K_o is related to the Elliptic integral of imaginary argument. The quantity a is related to η_o through the biquadratic equation:

$$1 - \eta_o^2 - \frac{1}{2}\left(\frac{\eta_o}{a}\right)^4 = 0 \qquad (4.16)$$

The differential da^2 can be expressed as $da^2 = \frac{da^2}{d\eta_o} \frac{d\eta_o}{d\sigma} d\sigma$ where $\frac{da^2}{d\eta_o}$ is obtained from equation (4.16) while $(d\eta_o/d\sigma)(\sigma)$ is obtained through inversion of equation (4.15).

This inversion can best be accomplished by defining a new variable $\alpha = 1 - \eta_o^2$ and solving equation (4.15) in the new form

$$\alpha = 1 - \left[\frac{\cos^{-1}\sqrt{\sigma}}{K_o(\alpha)}\right]^2 \qquad (4.17)$$

by iteration. Since α only varies between 0 and 1, $K_o(\alpha)$ can be easily evaluated by the power series

$$K_o(x) = \frac{\pi}{2} \sum_{n=0}^{\infty} \left(\frac{(2n-1)!}{n!\,(n-1)!\,2^{2n-1}} \right)^2 (-x)^n \qquad (4.18)$$

Since $K_o(\alpha)$ is a slowly varying function of α for the range of α considered, the solution converges rapidly.

By noticing that the integrand of $da^2(\sigma)$ is symmetric around $\sigma = \frac{1}{2}$ (i.e. replacement of σ by $(1-\sigma)$ leaves the integrand unchanged) we can fold the integration over by integrating from 0 to $\frac{1}{2}$ over both σ and $\sigma^1 = (1-\sigma)$ and adding the two parts. By changing σ^1 back to σ we can express the differential da^2 as

$$da^2(\sigma) = \left[\frac{\sqrt{1-\alpha}\,(1+\alpha)}{\alpha^{3/2}(K_o(\alpha) - 2K_1(\alpha)} + \frac{\sqrt{\beta}\,(2-\beta)}{(1-\beta)^{3/2}(K_0(1-\beta) - 2K_1(1-\beta))} \right] \cdot \frac{d\sigma}{2\sqrt{2\sigma(1-\sigma)}} \qquad (4.19)$$

where β is defined by the solution of the equation:

$$\beta = \left[\frac{\sin^{-1}\sqrt{\sigma}}{K_o(1-\beta)} \right]^2 \qquad (4.20)$$

while K_1 is related to K_o by the relation:

$$K_1(x) = (1-x)\frac{dK_o}{dx} = -\frac{\pi}{2}(1-x) \sum_{m=0}^{\infty} \left(\frac{(2m+1)!}{m!\,2^{2m+1}} \right)^2 \frac{(-x)^m}{m!\,(m+1)!} \qquad (4.21)$$

Since the relation between da^2 and $d\sigma$ is only an expression of the geometry of inverse fifth power particle interaction it can be determined independently of the problem under consideration. This just leads to the transformation of the integral

$$\int_0^{\infty} I(\sigma(a^2))\, da^2 = \int_0^{\frac{1}{2}} I(\sigma)\, WC(\sigma)\, d\sigma \qquad (4.22)$$

where I is any integrand and $WC(\sigma)$ is a numerically evaluated function dependent only on the choice of fifth power interaction law. One can now, in principle, evaluate the collision integral JN_o and JT_o numerically for the problem under consideration. It is more convenient, however, in the calculations of the moments to leave this σ integration until all the other integrations have been accomplished. In studying the nature of the collision integral, let us look at the integration of JN_{ol}, for instance. As $\sigma \rightarrow 0$ da^2 behaves as $C_1 d\sigma/\sigma^{5/4}$ (from equation 4.15, 4.19 and the definition of α) while the leading term of the rest of the integrand behaves as $C_2(\sqrt{\sigma}/(N - v_x))\, e^{-((N - v_x)/\sqrt{2\sigma})^2}$ for $|N - v_x| > \sqrt{2\sigma}$. Thus for all finite $|N - v_x|$ the integral is convergent. As $|N - v_x| \rightarrow 0$ the integrand has a sharp peak near $\sigma \approx |N - v_x|^2$ and can be approximately integrated in the above form to give the answer that

$$JN_{ol} = \frac{C_3 \text{ sign } (N - v_x)}{\sqrt{|N - v_x|}} + \text{h. o. t. } \ldots \qquad (4.23)$$

The other terms of the collision integral can be shown to contain the same type of singularity.

The collision integral, therefore, for Maxwellian molecules behaves very differently near $v_x = N$ than does the Krook model. This behaviour is physically explainable and reasonable. The Krook model by assuming spherical symmetry in the scattered particles restricts any pecularities around $v_x = N$ to come from the loss term alone. In the Maxwellian molecule collision integral (as for any power law interaction) the change in ff_1 through a collision is finite even for a very small deflection in a collision for $v_x \Longrightarrow N$, while the number of such collisions is approaching infinity. Thus near $v_x - N = 0$ the collision integral diverges.

This divergence is not real, as it is a result of the breakdown of the validity of the Boltzmann equation in the region of $v_x \longrightarrow N$. In this regime (near the initial discontinuity) the lack of a cutoff distance for interactions violates the binary collision assumption. Physically this can be considered as a result of the unrealistic initial conditions for the Boltzmann equation. The instantaneous removal of the diaphragm is inconsistent with the Boltzmann equation, as no times shorter than the duration of an average "collision" can be treated by the theory. Conceptually the divergent results can be eliminated by introducing a "thin adjustment layer"

(of the order of a collision time) into the initial conditions to replace the discontinuity. Fortunately this need not be done in detail as the physically meaningful results, the moments, are finite because of the integrable nature of the singularity.

The quantities JN_o and JT_o are constructed from JN_{ol}, JN_{os}, JT_{ol} and JT_{os} by substituting into the formulas

$$JN_o = \frac{(1 - \rho_r)}{2} JN_{ol} + \left(\frac{1 - \rho_r}{2}\right)^2 JN_{os}$$

$$JT_o = \left(\frac{1 - \rho_r}{2}\right) JT_{ol} + \left(\frac{1 - \rho_r}{2}\right)^2 JT_{os} \qquad (4.24)$$

The distribution function $f_1(N)$ can be evaluated in a fashion identical to that used in the Krook model calculation. Equation 2.12, however, indicates that around $v_x = N$, f_1 will have the singularity of J_o. Thus f_1 based on Maxwellian molecules will also differ in this region from f_1 evaluated on the basis of the Krook model. Figure 4 is a map of f_1 in the v_x, N plane. For $|v_x - N| \longrightarrow \infty$ the distribution function looks very similar to that obtained by the Krook model, though near $v_x = N$ the behaviour is of course quite different. From the comparison of the two solutions in Figure 6 it is evident that any moment (integral over v_x) cannot be strongly dependent on which distribution function is used. Not only is the region of great discrepancy between the two solutions confined to a relatively narrow region around $v_x = N$, but also the contributions to the total area from opposite sides of $v_x = N$ cancel out.

As already mentioned, for computational reasons it is more convenient to carry out the integration over v_x and N^1 first and do the geometric integration over the collision parameter σ last. Figure 5 shows a typical contribution to a moment plotted as a function of the half angle between the asymptotes of collision. It is evident that no singularity exists in this last integration.

The fact that the collision integral is a sum of two terms (linear and quadratic in $(1 - \rho_r)/2$ allows computation of the moments for these two terms independently of the initial density ratio ρ_r, and then synthesizing a solution for any ρ_r by properly combining the two terms.

The numerical techniques for evaluating the moments are very similar to those used in evaluating the Krook model solution. The integrations over v_x and N^1 are carried out in identical fashion. The integration over v_{x_1} required in the quadratic terms of the collision integral is carried out by separating regions where analytical integration can be carried out from those where it cannot. The direct use of a Gaussian quadrature in the numerical region and the addition of the contributions from the analytically available regions gives the total integrations. This step was essential because of the great dependence of the integrand on three parameters other than the variable of integration. The final integration over σ is carried

out by a Lobatto (Radau (1880)) or Gaussian (Lowan, Davids, and Levenson (1942)) quadrature. Since this procedure specifies the points σ_i at which the integrand has to be evaluated independently of any other parameter, $da^2/d\sigma$ was evaluated at those points independently of v_x, N or initial density ratio.

The accuracy of the integrations was checked by changing the types and orders of the quadratures at some selected points. A further check on the proper evaluation of the collision integral was obtained by taking the first three moments of J_o and comparing them with the same moments of f_1. This procedure is in effect a check on the three conservation relations which the collision integral must satisfy. A similar check can be obtained by comparing the integral

$$\int_{-\infty}^{\infty} v_x^2 JN_o dv_x \quad \text{with} \quad \int_{-\infty}^{\infty} JT_o dv_x$$

as their sum should be zero in order to conserve energy.

All the checks yield the answer that the methods employed here are accurate to within about a percent in the bulk of the cases. The limiting case of solutions at large N for $\rho_r \longrightarrow 0$ causes some additional complications, because the final answers are obtained by taking differences between two large numbers to obtain a small number. The accuracy in the moments there must therefore be much better to yield accurate physical variables.

The points in that regime therefore required higher order quadratures to retain reasonable accuracy. This difficulty in the extensive properties such as density or pressure is unimportant because the general level there is itself small. The intensive properties such as temperature and velocity, however, can be appreciable in just those regions.

V. RANGE OF VALIDITY OF SOLUTION

Though no general discussion of the validity of the solution is possible, the only possible solution separable in the coordinates $\mathcal{Y}$ and N satisfying the requirement of finiteness at $\mathcal{Y} = 0$ is the power series in $\mathcal{Y}$ obtained in Section II. This discussion is carried out in detail in the Appendix. This result means that if such a separable solution is valid the first order effect of collisions is linear in $\mathcal{Y}$.

Since $f_1 (v_x, N)$ for the case of the Maxwellian molecule collision integral is singular at $v_x = N$ the function f_1 becomes infinite and the perturbation scheme fails. This difficulty, however, has already been discarded in the previous section as a result of the initial conditions being inconsistant with the Boltzmann equation in this region of the v_x, N plane. Conceptually the singularity can be removed by the introduction of an adjustmant layer either in the initial conditions or in the solution in the region where the Boltzmann equation fails. Since the contribution of this region to the physically meaningful moments is negligible this difficulty can be avoided.

Even after the elimination of the singularity no precise mathematical derivation of the region of convergence is possible without knowledge of the general n'th term in the expansion.

We are forced therefore to resort to less rigorous means of determining the possible regions of validity. If we concentrate our attention on only the first order term in the expansion we can get some estimate of the range of its validity by looking at its ratio to the zeroth term. This procedure is based on the requirement that the first order effect remain a small perturbation.

Possibly a better procedure is to evaluate the next higher order term and limit the validity of the first order solution to regions where the second order term is negligible. Unfortunately even an estimate of this term can be obtained only for the Krook model case and not for the "exact" case.

In the "exact Maxwellian molecule" case we are forced to resort to the first method. Figure 6 represents some typical cases of the ratio FN_1/FN_o. If we limit the validity of the solution let us say to $FN_1\mathscr{T}/FN_o = .1$ then we can obtain the maximum time that the solution, with this first order term alone, could be valid as

$$\mathscr{T}_m = .1/(FN_1/FN_o) \qquad 5.1)$$

Neglecting the fictitiously singular region near $v_x = N$ we can choose $\mathscr{T}_m \approx 1$ for $|v_x| < 2.5$. For $|v_x| \to \infty$, the ratio FN_1/FN_o is proportional to v_x and thus diverges.

This, however, is unimportant as the moments are obtained by integrating with an $\exp(-v_x^2)$ weighting function which makes this region contribute little to the total integrals. The same difficulty appears in the Chapman-Enskog procedure, (the distribution function can get negative for $|v_x|$ large) without seriously limiting the validity of the results.

Figure 7 represents a typical example of the ratio of the moments. Here again it is apparent that if we base validity of solution on the ratio $v_1\tau/v_o \leq .1$ the maximum time $\tau_m \approx 1.0$ except when $|N| \longrightarrow \infty$. The solution in that region, however, is of little interest, since both the collisionless and the perturbation solutions are essentially zero, even if their ratio is high.

In the case of the Krook model solution we can get an additional check on the validity by estimating the order of magnitude of the second order term f_2. At a point $v_x = N$, $FN_1 = JN_o$ and $FN_2 = JN_1/2$, we have only to obtain JN_1 from the Krook model to get an estimate of the maximum value of FN_2.

Now JN_1 is:

$$JN_1 = \left(\chi_1 + \frac{\rho_1}{\rho_o}\right) FN_1 + \rho_o(\chi_1 FN_o - FN_1) \qquad (5.2)$$

where $$\chi_1 = \left(\frac{\rho_1}{\rho_o} + 2u_1 \frac{(v_x - u_o)}{T_o}\right) + \frac{T_1}{T_o} \frac{(v_x - u_o)^2}{T_o} - \frac{1}{2} \qquad (5.3)$$

Though it is hard from this expression to deduce the general nature of the JN_1 term a few calculations convince one that $-\rho_o FN_1$ is the leading term, and that therefore $|FN_2/FN_1|$ at the point of discontinuity is always less than $\frac{1}{2}$. ($FN_2 \approx \frac{1}{2} JN_1 + \ldots$). Also since JN_1 is of the order of JN_o or less, and the integral for FN_2 has a faster decay in $(v_x - N)$ (because of the $1/(v_x - N)^3$ term) away from $v_x = N$, the ratio $|FN_2/FN_1|$ would be expected to decrease somewhat faster than FN_1/FN_o. We can therefore say that in general $|FN_2/FN_1|$ is less than $|\rho_o/2|$ and far from the line $v_x = N$ probably considerably below that value. A few graphical calculations indicate that $|FN_2/FN_1|$ over most of the v_x, N plane is of the order of .1, just like $|FN_1/FN_o|$. This result suggests that when $FN_1\mathcal{V}/FN_o \approx .1$, neglecting the second order term even at $\mathcal{V} \tilde{\Rightarrow} 1$ is justified to within a few percent.

Though the same type of analysis cannot be carried out for the "exact" case the similarity of the solutions between the two cases in the first order term suggests that probably the same type of result holds for the "exact" case.

Unfortunately these statements about the order of magnitude of the corrections in the distribution function cannot be easily translated into orders of magnitude of the corrections to the moments without actually solving the problem. The basically similar behaviour of JN_1 and JN_o suggests, however, that the overall ratio of the moments should be of the same order as (FN_2/FN_1), though locally in certain regions this statement might not be true, especially at the zero's of first order moments.

VI. RESULTS AND CONCLUSIONS

As explained in Sections III and IV, the macroscopic properties of density, pressure, temperature, velocity, stress and heat flux were calculated numerically for both the Krook model and the "exact" Maxwellian molecule case, for the case of equal initial temperature on the two sides of the diaphragm. The initial density ratios for the calculations were chosen by picking cases that would yield certain shock Mach numbers in the Euler limit. The cases of $M_s \longrightarrow 1.0$, $M_s = 1.27$, $M_s = 2.0$ and $M_s = 3.0$ were calculated in detail. The case $M_s \longrightarrow 1.0$ was chosen to illustrate the linearized limit. The $M_s = 1.27$ case was chosen because the shock pressure rise normalized by the high pressure p_- is a maximum there. The $M_s = 3.0$ case was the largest Mach number for which calculations could be carried out without necessitating double precision on the computer or more complicated numerical techniques. For a cold shock tube ($T_- = T_+ = T$) at $\gamma = 5/3$ the limiting shock Mach number for infinite pressure ratio is only $M_s = 4.24$; thus extension of the solution from $M_s = 3.0$ to this limit was not considered useful. The $M_s = 2.0$ case was calculated in order to have an intermediate point.

The density profiles for collisionless flow ρ_o, the Euler solution ρ_e, and the first collision perturbation ρ_1 for both collision models for three Mach numbers are represented in Figure 8a, b, c. Figures 9, 10, and 11 are similar plots for pressure, stress and heat flux. In all these figures the results for $M_s = 2.0$ are omitted, because all the difference between the $M_s = 2.0$ and $M = 3.0$ cases occur in the region of low density ($N >> 1$), and are therefore negligible compared to the main disturbance. Figures 12 and 13 are similar plots of velocity and temperature, respectively, for all the Mach numbers calculated. Since these two properties are normalized by density the regions of low density are not attenuated and can thus be of great importance. Figure 14 is an expanded view of the velocities normalized by the initial density difference for all the calculated Mach numbers in the vicinity of the eventual shock formation.

It is apparent that for all the evaluated macroscopic properties the qualitative appearance of the first order term (linear in time) is very similar for both the Krook and the "exact Maxwellian" model. Quantitatively, however, the discrepancy between the two solutions is not constant either for different moments or at different positions ($N = x/c_o t$). Because of the single free parameter in the Krook model the accuracy of the

different moments cannot be expected to be the same. The qualitative agreement is therefore surprisingly good. In view of the greatly different type of singularity of the distribution function obtained by the two methods, the great qualitative agreement between the macroscopic moments is an indication of the insensitivity of the macroscopic properties to the details of the collision process, as long as the basic conservation laws are satisfied. The macroscopic properties including moments which have v_t^2 in the integrand appear to have a greater difference between the Krook and the exact solution than do those with moments of the v_x velocity only. This is most noticeable in the linearized case by comparing velocity and temperature profiles, where the difference between the two solutions for the velocity is approximately 30% at the peaks, while for the temperature it is closer to 100% . This suggests that possibly the spherical symmetry inherent in the Krook collision model represents themalization incorrectly by assuming it to be equal in all directions around the mean velocity.

Another important discrepancy between the Krook and the exact solution is the apparent dependence of the difference between these solutions in the low density region on the initial density ratio. The velocity profiles in Figure 14 indicate that the discrepancy is growing with Mach number. Comparison

between the Euler and collisionless solution (Figure 2) shows that whereas on the high density side the two velocity profiles are fairly close regardless of the Mach number, in the region near the eventual shock formation the discrepancy grows with Mach number. Since the Euler solution is based on local equilibrium, the close proximity to it of the collisionless solution suggests that in the high density region the assumption of near equilibrium inherent in the justification of the Krook model may be reasonably correct. Near the shock formation region, however, this assumption becomes less and less reasonable as the eventual shock Mach number is increased.

In general we can conclude that at least for the problem where the initial temperature is the same on both sides of the diaphragm the Krook model gives a reasonable gross description of the initial effect of collisions. Since the Krook model is known to be correct (within the limitations of the one free parameter) as equilibrium is approached, its use for numerical studies in the transition range of problems similar to this one seems justified. The limitations of the validity in the eventual shock formation region and the apparent incorrect thermalization suggest that the use of the model in problems with collisions between streams of greatly differing velocities and temperatures may be unjustified, or at least less accurate.

Regardless of which solution we use we have now enough information to indicate at least the direction in which the profiles of the macroscopic moments will be altered initially as a result of collisions. Figure 15 represents a typical plot of the expected temperature profiles at various times as a function of $N = x/a_o t$. In addition to the limiting cases of collisionless and Euler solutions, profiles at $\tau = 1$ and $\tau = 3$ are obtained by adding the first collision solution, although the validity of the solution at $\tau = 3$ is doubtful. To make comparison to the large time solution more meaningful a crude approximation to the Navier-Stokes solution is evaluated for $\tau = 100$ and $\tau = 50$. This approximation consists of neglecting all interaction between the shock, the contact surface and the expansion wave. The shock, however, is modified to be the equilibrium shock profile for a steady normal shock (Gilbarg and Paolucci (1953)). The contact surface is modified to include the heat conduction and viscosity as done by Golworthy (1959). The expansion wave is very crudely calculated by modifying a linearized solution for a wave front. In a linearized theory an equilibrium wave front for the temperature would be modified by viscosity and heat conduction into an error function, which in our variables would look as follows

$$T = \frac{(T_- + T_e)}{2} - \frac{T_- - T_o}{2} \operatorname{erf}\left(b\sqrt{\tau}\,(a_o + c_o N)\right) \qquad (6.1)$$

where T_- is the temperature on the high pressure side, T_e is Euler solution temperature on the low pressure side of the expansion wave, b is a constant dependent on the undisturbed kinematic viscosity and Prandtl number, and a_o is the unperturbed speed of sound. For the non-linear problem the form was assumed to remain the same but b, a_o and c_o were assumed to be functions of N based on the Euler solution. Though this cannot be expected to be a correct solution the "thickness" of the wave has the correct growth in time, and the general order of magnitude should be correct.

At $\mathcal{P}$ = 50 the "non-interacting" Navier-Stokes approximation is at the absolute limit of its possible validity, because the region separating the shock and contact surface is very small compared to their thicknesses. The process of transition appears more or less direct and no really new phenomena can be expected to occur between $\mathcal{P}$ = 3 and $\mathcal{P}$ = 50. The mathematical forms of the two limiting solutions are, however, vastly different. Inclusion of interaction in the Navier-Stokes solution would reduce the gap of uncertainty even further, and together with the first collision results would probably be adequate to describe the complete process of propagation of an initial density discontinuity.

A look at the various other macroscopic variables (Figures 8 to 13) shows that in general the initial effect of collisions is to alter the profiles in the proper direction towards the Euler

solution. What appears initially as an incorrect direction for the velocity perturbation (Figure 12) in the "contact surface" region, becomes reasonable when one refers back to Figure 1 and notices that the Navier-Stokes perturbation is also in the same direction. The temperature perturbation (Figures 13 c, d) in the "contact surface" region for the high Mach number cases likewise appears to be in the wrong direction. Aside from the dubious meaning of temperature for non-equilibrium flows the apparent excessive cooling in that region can be made plausible by noticing that the cooling comes from the high density region, where collisions become important earlier that in the "shock" region where heating is expected to occur.

Figure 16 is a plot of the heat flux distribution for $\mathcal{P} = 0$, 1 and 3 based on the present first collision perturbation, compared to the same crude Navier-Stokes approximation of Figure 15 for $\mathcal{P} = 50$ and 100. Neglecting some difficulties in the regions of $|N| \gg 1$, the general trend is to reduce the heat flux levels and make them qualitatively similar to the Navier-Stokes distributions. The fact that the heat flux level is being quickly reduced except in certain regions suggests that the Navier-Stokes equations should become valid in only a few mean free times.

The stress-velocity gradient and heat flux-temperature gradient relations have the same form in both continuum and collisionless cases (except for the time dependence of the coefficients in the latter) (Narasimha (1961)). This suggests that a good representation of the process of transition from collisionless to collision dominated flow can be obtained by looking at the ratio

$$\left(\frac{P_{xx}}{-\frac{4}{3}\mu\frac{\partial u}{\partial x}}\right) \qquad \text{or} \qquad \left(\frac{q_x}{-K\frac{\partial T}{\partial x}}\right)$$

as a function of time. These two quantities evaluated on the basis of the first collision perturbation in the linearized case are presented in Figure 17. The perturbation appears to be in the right direction. Its form suggests that the assumption of a time dependent viscosity (or heat conductivity) of the form

$$\mu = \mu_{N.S.}\,(1 - e^{-a\mathscr{R}}), \tag{6.2}$$

where $\mu_{N.S.}$ is the usual viscosity and a is a constant, could be a useful means of obtaining a complete solution within the Navier-Stokes formalism. This technique has the advantage of going to the proper limits correctly while using only a single set of equations.

In the non-linear case calculation of a similar ratio of stress to velocity-gradient (or heat flux to temperature gradient) becomes complicated by the fact that in the first approximation the ratio can become infinite, because the numerator and denominator do not vanish simultaneously. The stress to velocity gradient ratio is shown in Figure 18 for the $M_s = 2.0$ case. The much stronger dependence of the perturbation on position ($N = x/c_o t$) is evident. The perturbation changes sign around the regions of the "contact surface" and the shock. It also becomes infinite in the vicinity of the "contact surface". This is just a result of the fact that the first order perturbation does not go to zero at the same point as the collisionless solution. Fortunately this difficulty occurs just in those regions where the stress is zero and thus the stress-rate of strain relation is unimportant. An assumption of a time dependent viscosity or heat conductivity as in Equation (6.2) might be less accurate than in the linear case but certainly would still retain the gross features of the problem.

All the results of the first collision perturbation suggest that a large fraction of the phenomena occuring in the transition to the Euler solution will occur in a region where Navier-Stokes equations are valid. This does not mean, however, that the solution will be in general obtainable by considering a separate shock, contact surface and expansion wave which have their own

viscous structures but which do not influence each other. Unfortunately this interaction makes the problem very difficult in the non-linear case. Presently the linearized solution of the Navier-Stokes equation is being calculated for this problem. Later extension of at least the basic features of the interaction to the non-linear problem, coupled with the present short-time solution should adequately describe the propagation of an initial density discontinuity.

REFERENCES

Bhatnager, P. L.; Gross, E. P.; and Krook, M.: A Model for the Collision Processes in Gases. I. Small Amplitude Processes in Charged and Neutral One-Component Systems. Physical Review, Vol. 94, No. 3, pp. 511 - 525, May 1, 1954.

Broadwell, J. E.: Study of Rarefied Shear Flow by the Discrete Velocity Method. Space Technology Lab. Rept. 9813-6001-RU000, March, 1963. (Paper to appear in Journal of Fluid Mechanics; also paper to be presented at 4th Rarefied Gas Dynamics Symposium, Toronto, Canada 14-17 July, 1964.)

Gilbarg, D.; and Paolucci, D.: The Stucture of Shock Waves in the Continuum Theory of Fluids. Journal Rational Mechanics and Analysis, Vol. 2, pp. 617-642, 1953.

Glass, I. I. : Shock Tubes. I. Theory and Performance of Simple Shock Tubes. University of Toronto, Institute of Aerophysics Review No. 12, May 1958.

Goldworthy, F. A.: The Structure of a Contact Region, with Application to the Reflection of a Shock from a Heat-Conducting Wall. Journal of Fluid Mechanics Volume 5, Part 1, pp. 164-170, January 1959.

Haviland, J. K. and Lavin, M. L.: Application of the Monte Carlo Method to Heat Transfer in a Rarefied Gas. Physics of Fluids, Vol. 5, No. 11, pp. 1399-1405, November 1962.

Jeans, J. H.: The Dynamical Theory of Gases (4th Edition). Dover Publications, Inc., New York, N. Y., 1954. Chapter VIII. pp. 213-217.

Keller, J. B.: On the Solution of the Boltzmann Equation for Rarefied Gases. Communications on Pure and Applied Mathematics, Vol. 1, pp. 275-285, September, 1948.

Krook, M.: Continuum Equations in the Dynamics of Rarefied Gases. Journal of Fluid Mechanics, Vol. 6, Part 4, pp. 523-541, November 1959.

Lavin, M. L.: A Monte Carlo Solution for Heat Transfer in Rarefied Gases. M. I. T. Fluid Dynamics Research Laboratory Report No. 61-3, May 1961.

Lees, L.: A Kinetic Theory Description of Rarefied Gas Flows. Memorandum No. 51 - Hypersonic Research Project - Guggenheim Aeronautical Laboratory, California Institute of Technology, December 1959.

Lowan, A. N.; Davids, N.; and Levenson, A.: Tables of Zeros of the Legendre Polynomials of Order 1 - 16 and the Weight Coefficients for Gauss's Mechanical Quadrature Formula. Bulletin of American Mathematical Society, Vol. 48, pp. 739-743, 1942.

Narasimha, R.: Collisionless Expansion of Gases into a Vacuum. Journal of Fluid Mechanics, Vol. 12, pp. 294. February 1962.

National Bureau of Standards Applied Mathematics Series: Tables of Functions and Zeros of Functions. Vol. 37, U. S. Government Printing Office, Washington, D. C., 1952.

Patterson, G. H.: Theory of the Shock Tube. Naval Ordnance Laboratory Memorandum No. 9903, 1948.

Radau, R.: Etude sur des Formules d'Approximation qui servent a Calculer la Valeur d'une Integrale Definie. Journal de Mathematiques Pures et Appliques, Tome VI, Series 3, pp. 283-336, 1880.

Willis, D. R.: On the Flow of Gases under Nearly Free Molecular Conditions. Princeton University Gas Dynamics Laboratory, Report No. 442, December 1958.

Willis, D. R.: Investigation of the Development of a Shock Wave for Times Smaller than the Average Collision Time. Royal Institute of Technology, Stockholm. Division of Gas Dynamics Technical Note No. 4, December 1960. ASTIA No. 254995.

APPENDIX

The Boltzmann equation in the transformed, non-dimensional variables has the form (Eq. 2.9):

$$\mathcal{T} \frac{\partial f}{\partial \mathcal{T}} (v, N, \mathcal{T}) + (v_x - N) \frac{\partial f(\vec{v}, N, \mathcal{T})}{\partial N} = \mathcal{T} J(f, \vec{v}, N, \mathcal{T}) \qquad (A-1)$$

where J is the collision term, non-linearly dependent on $f(v, N, \mathcal{T})$ for both the exact collision integral and the Krook model. We now look for solutions which are separable in the variables $\mathcal{T}$ and N (where v is just a parameter), and which are finite at $\mathcal{T} = 0$. The procedure can best be illustrated by calculating the first time-dependent terms and then generalizing to an infinite series.

We assume that a separable solution of the form:

$$f(v, N, \mathcal{T}) = f_o(\vec{v}, N) + g_1(\mathcal{T}) f_1(\vec{v}, N) + g_2(\mathcal{T}) f_2(\vec{v}, N) + \ldots \qquad (A-2)$$

exists and is finite at $\mathcal{T} = 0$. The terms are assumed to have been ordered in such a way that $g_1(\mathcal{T})$ is the leading time-dependent term for small $\mathcal{T}$. It can be readily verified that this form for f yields a similar form for J. Thus $J(f, v, N, \mathcal{T})$ can be expressed as

$$J(f, v, N, \mathcal{T}) = J_o(f_o, v, N) + h_1(\mathcal{T}) J_1(f_o, f_1, v, N) + h_2(\mathcal{T}) J_2(f_o, f_1, f_2, v, N) + \ldots \qquad (A-3)$$

For the exact collision integral substitution of f as expressed by equation (A-2) yields the relation between the h_1 and g_1, as well as the relations between J_o and f_o, and J_1 and f_o and f_1. Since the integration is performed over velocities only, the time dependence can be taken outside the integrals and

$$J_o(f_o,\ v,\ N) = \int_{-\infty}^{\infty}\int_{0}^{2\pi}\int_{0}^{\infty} (f_o^{1},\ f_{o_1}^{\ 1} - f_o f_{o_1})\ \left|\vec{v} - \vec{v}_1\right|\ bdbd\varepsilon\ d^3\vec{v}_1 \qquad (A\text{-}4)$$

while $h_1(\mathscr{C}) = g_1(\mathscr{C})$ and

$$J_1(f_o,\ v,\ N) = \int_{-\infty}^{\infty}\int_{0}^{2\pi}\int_{0}^{\infty} (f_o^{1} f_{1_1}^{\ 1} + f_1^{1} f_{o_1}^{\ 1} - f_o f_{1_1}^{\ 1} - f_1 f_{o_1})\left|\vec{v} - \vec{v}_1\right|\ bdbd\varepsilon d^3 v_1 \qquad (A\text{-}5)$$

For the Krook model, evaluation of the macroscopic parameters by integration over velocity space yields

$$\begin{aligned}
\rho(N,\mathscr{C}) &= \iiint f(v,\ N,\mathscr{C})\ m d^3\vec{v} = \rho_o(N) + g_1(\mathscr{C})\rho_1(N) + g_2(\mathscr{C})\rho_2(N) \ldots \\
\rho v(N,\mathscr{C}) &= \iiint f(v,\ N,\mathscr{C})\ m v_x d^3\vec{v} = (\rho v)_o(N) + g_1(\mathscr{C})(\rho v)_1(N) + g_2(\mathscr{C})(\rho v)_2 \qquad (A\text{-}6) \\
E(N,\mathscr{C}) &= \iiint f(v,\ N,\mathscr{C})\ \frac{mv^2}{2}\ d^3\vec{v} = E_o(N) + g_1(\mathscr{C})\ E_1(N) + g_2(\mathscr{C})\ E_2(N)
\end{aligned}$$

By using Eq. (A-6) ρ, u, T for the Krook model can be also obtained as expansions in $g_1(\mathscr{C})$, $g_2(\mathscr{C})$ ... , and J is then evaluated again as an expansion in $\mathscr{C}$ with

$$J_o = c\mathscr{C} f_o \nu_o(N)\left[\frac{\rho_o(N)}{(2\pi R T_o(N))^{3/2}}\ \exp\left\{\frac{-(v_x - v_o(N)^2 + v_y^{\ 2} + v_z^{\ 2}}{2RT_o(N)}\right\} - f_o(N)\right] \qquad (A\text{-}7)$$

while $h_1(\mathcal{C})$ is again equal to $g_1(\mathcal{C})$ and J_1 involves f_o, f_1 and ρ_o, v_o, T_o, ρ_1, v_1, T_1. The Boltzmann equation can now be rewritten as:

$$(v_x - N)\frac{df_o}{dN} + g_1(\mathcal{C})\left[\frac{\mathcal{C}}{g_1}\frac{dg_1}{d\mathcal{C}} f_1 + (v_x - N)\frac{df_1}{dN} - \frac{\mathcal{C}}{g_1} J_o\right] +$$

$$g_2(\mathcal{C})\left[\frac{\mathcal{C}\, dg_2}{g_2\, d\mathcal{C}} f_2 + (v_x - N)\frac{df_2}{dN} - \frac{\mathcal{C} g_1}{g_2} J_1\right] + \ldots = 0 \qquad \text{(A-8)}$$

The solution for f_o is of course the collisionless solution given by equation 2.15. Now if we want the rest of the solution to be separable and satisfy the equation for all $\mathcal{C}$, the coefficients of $g_1(\mathcal{C})$, $g_2(\mathcal{C})$ etc. have to be independent of $\mathcal{C}$ and to be zero separately. The first equation

$$\frac{\mathcal{C}}{g_1}\frac{dg_1}{d\mathcal{C}} f_1 + (v_x - N)\frac{df_1}{dN} - \frac{\mathcal{C}}{g_1(\mathcal{C})} J_o = 0 \qquad \text{(A-9)}$$

$$\frac{\mathcal{C}}{g_1}\frac{dg_1}{d\mathcal{C}} = \text{const.} \quad \text{and} \quad \frac{\mathcal{C}}{g_1(\mathcal{C})} = \text{const.}, \qquad \text{(A-10)}$$

or,

$$g_1(\mathcal{C}) = A\mathcal{C} \qquad \text{(A-11)}$$

where A is arbitrary, while the equation for f_1 becomes

$$(v_x - N)\frac{df_1}{dN} + f_1 = \frac{J_o}{A} \qquad \text{(A-12)}$$

It is readily apparent that A can be chosen arbitrarily, since the product $g_1(\mathcal{E})\, f_1(v, N)$ is independent of A. We choose therefore to fix A as unity. Similar arguments for the coefficient $g_2(\mathcal{E})$ in equation (A-8) lead to

$$g_2(\mathcal{E}) = \mathcal{E}^2$$

and
$$(v_x - N)\frac{df_2}{dN} + 2f_2 = J_1 \qquad \text{(A-13)}$$

Extension of equations (A-2) and (A-3) to infinite series while retaining the condition of finiteness at $\mathcal{E} = 0$ yields the relations

$$g_n(\mathcal{E}) = \mathcal{E}^n \quad \text{for all } n \quad , \qquad \text{(A-14)}$$

while $f_n(v, N)$ satisfy equations 2.14 and 2.15 of the text. Thus the only solution separable in the variables $\mathcal{E}$ and N which corresponds to the collisionless solution at $\mathcal{E} = 0$ is the power series in $\mathcal{E}$ discussed in the text.

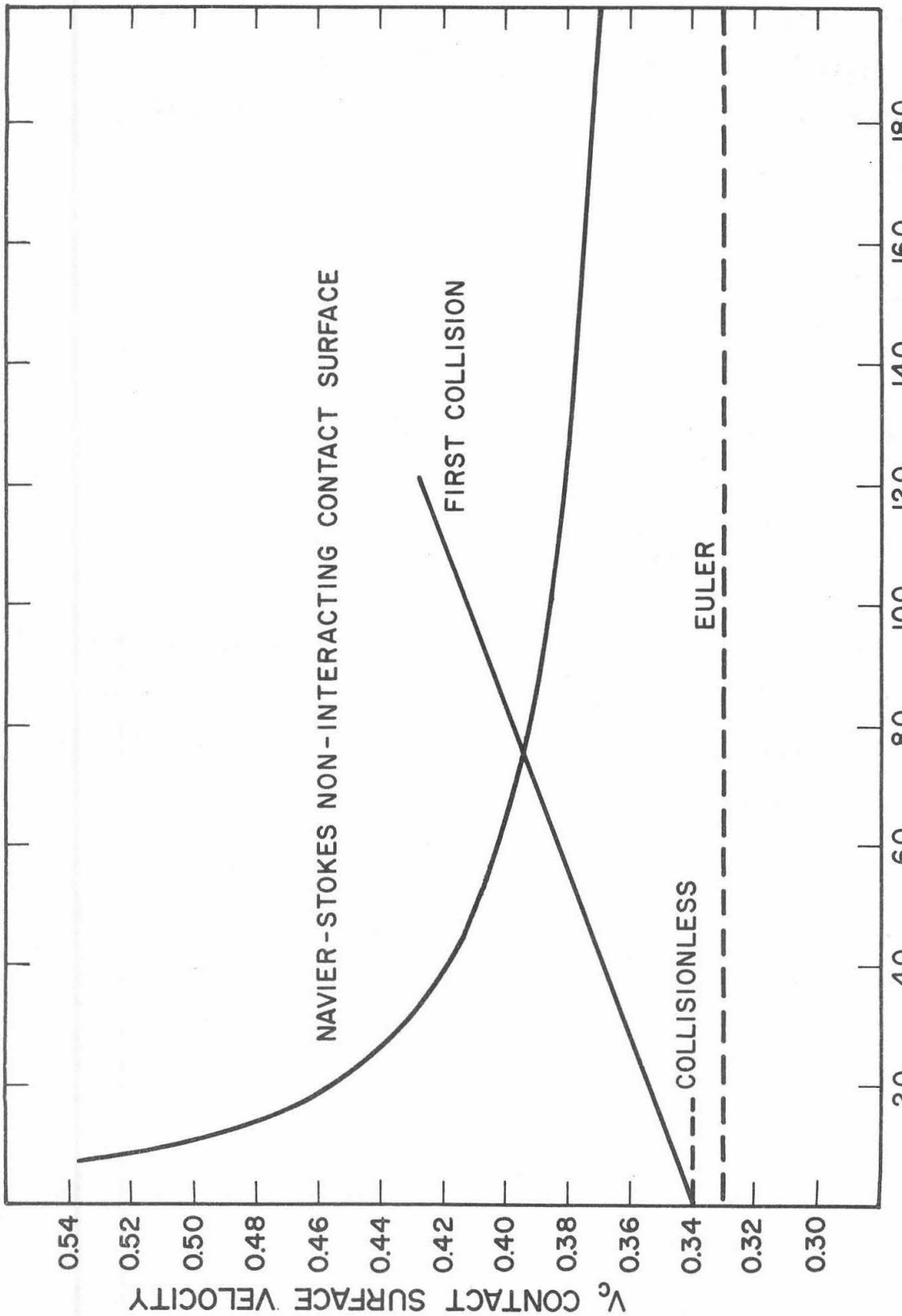

FIG. I - VELOCITY AT CONTACT SURFACE, ($M_s = 1.27$, $\rho_r = 0.298$)

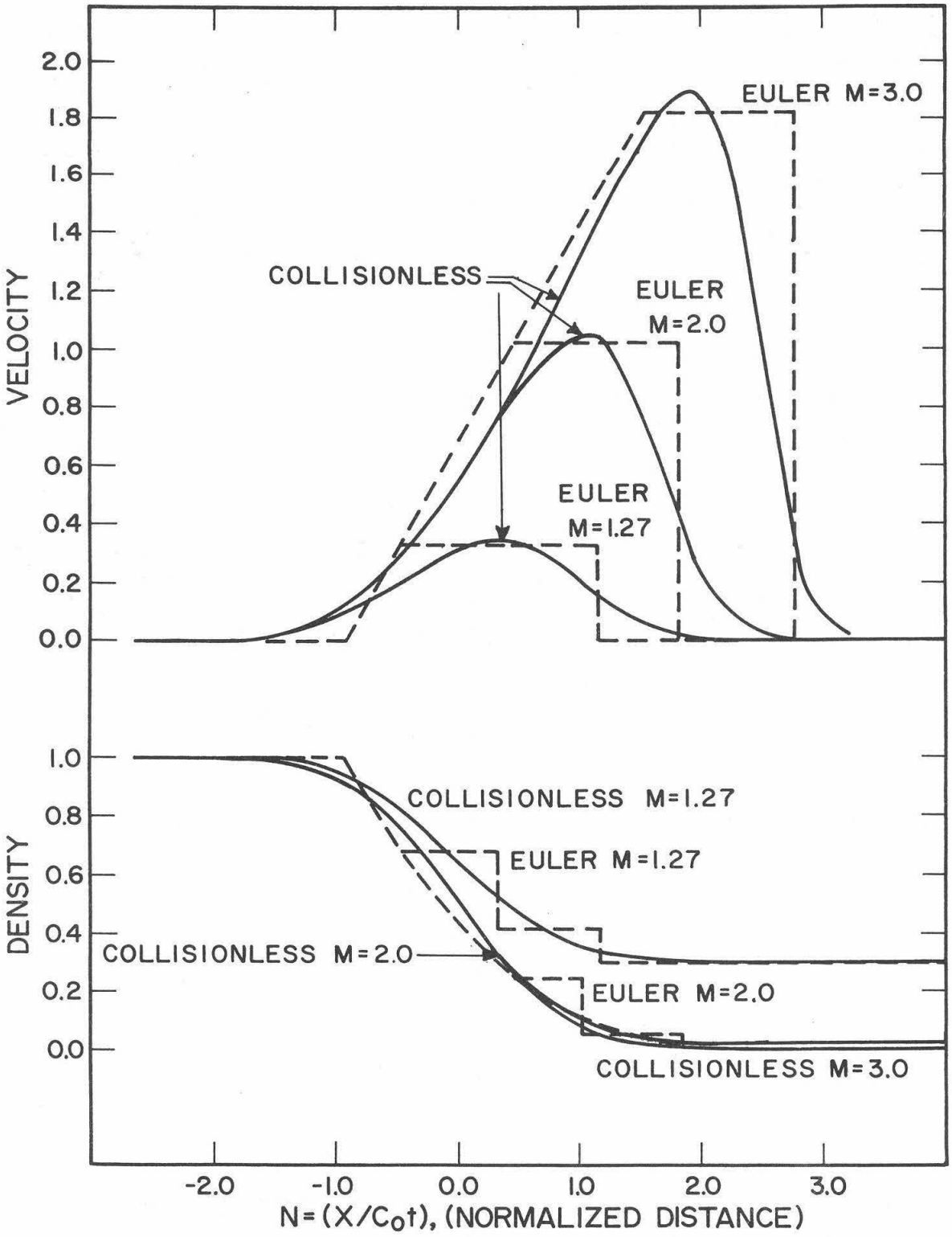

FIG.2 - LIMITING SOLUTIONS

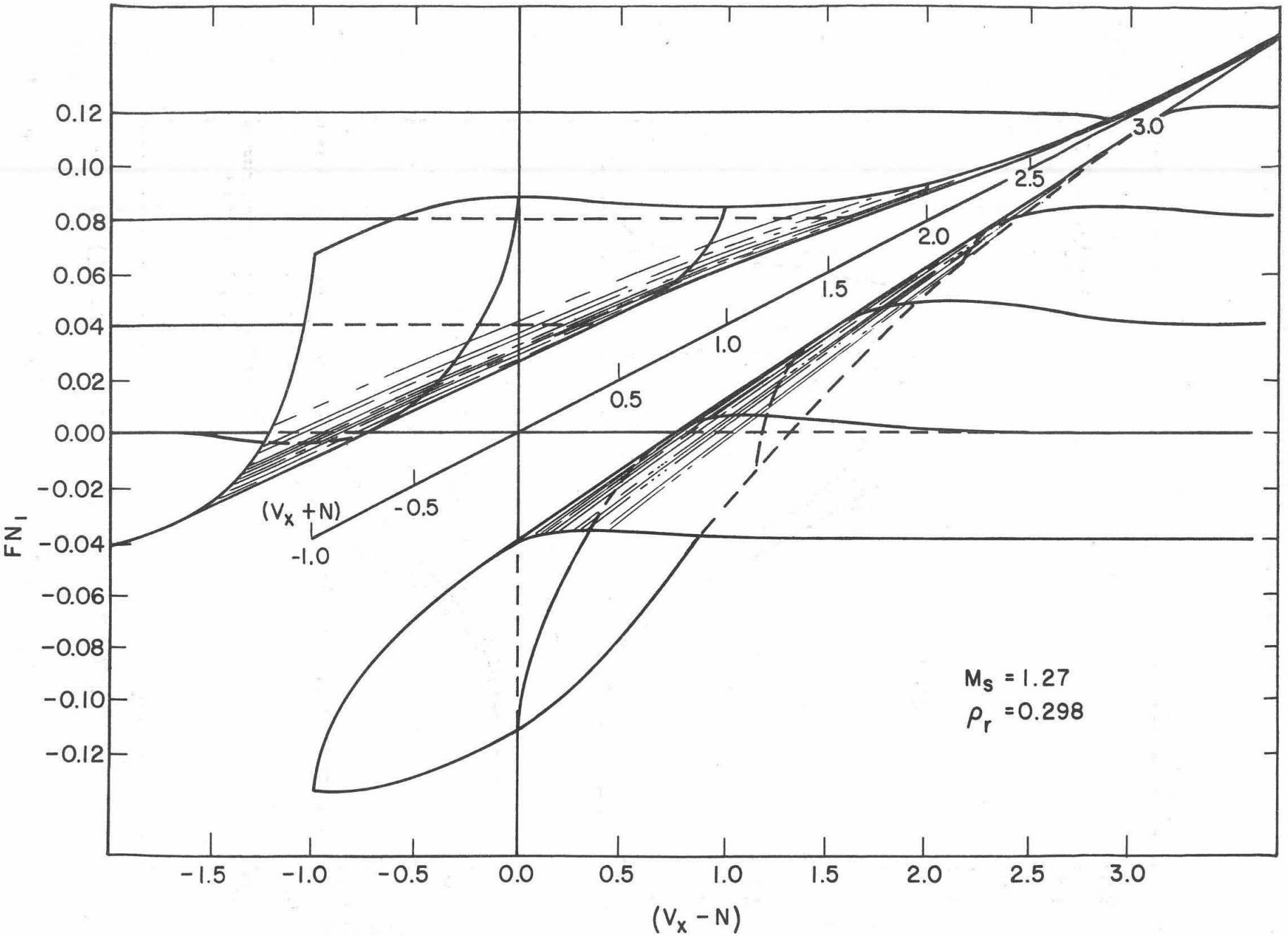

FIG. 3 - PERTURBATION DISTRIBUTION FUNCTION FN_1 FOR KROOK MODEL

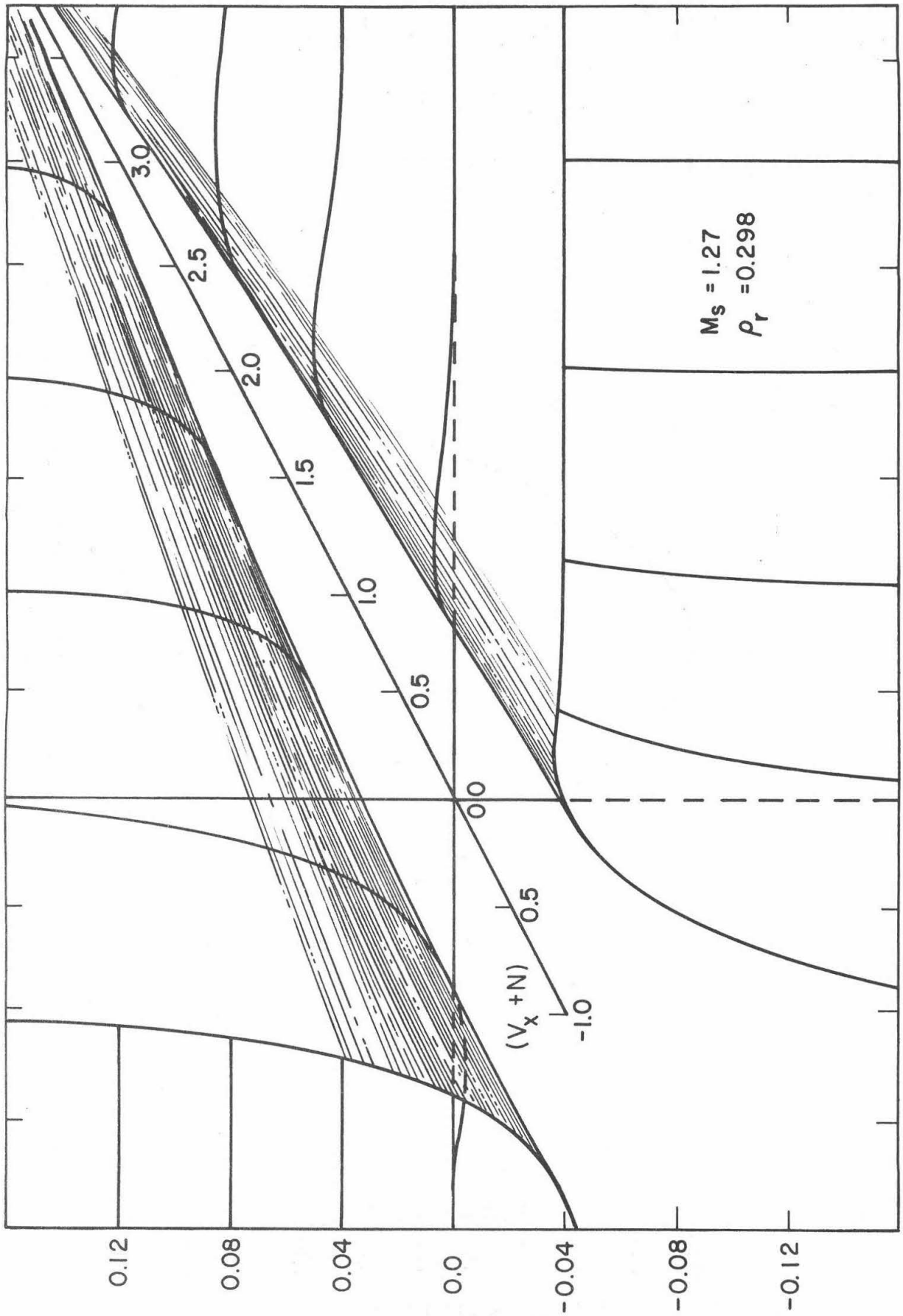

FIG. 4 – PERTURBATION DISTRIBUTION FUNCTION FN_1 FOR EXACT COLLISION INTEGRAL

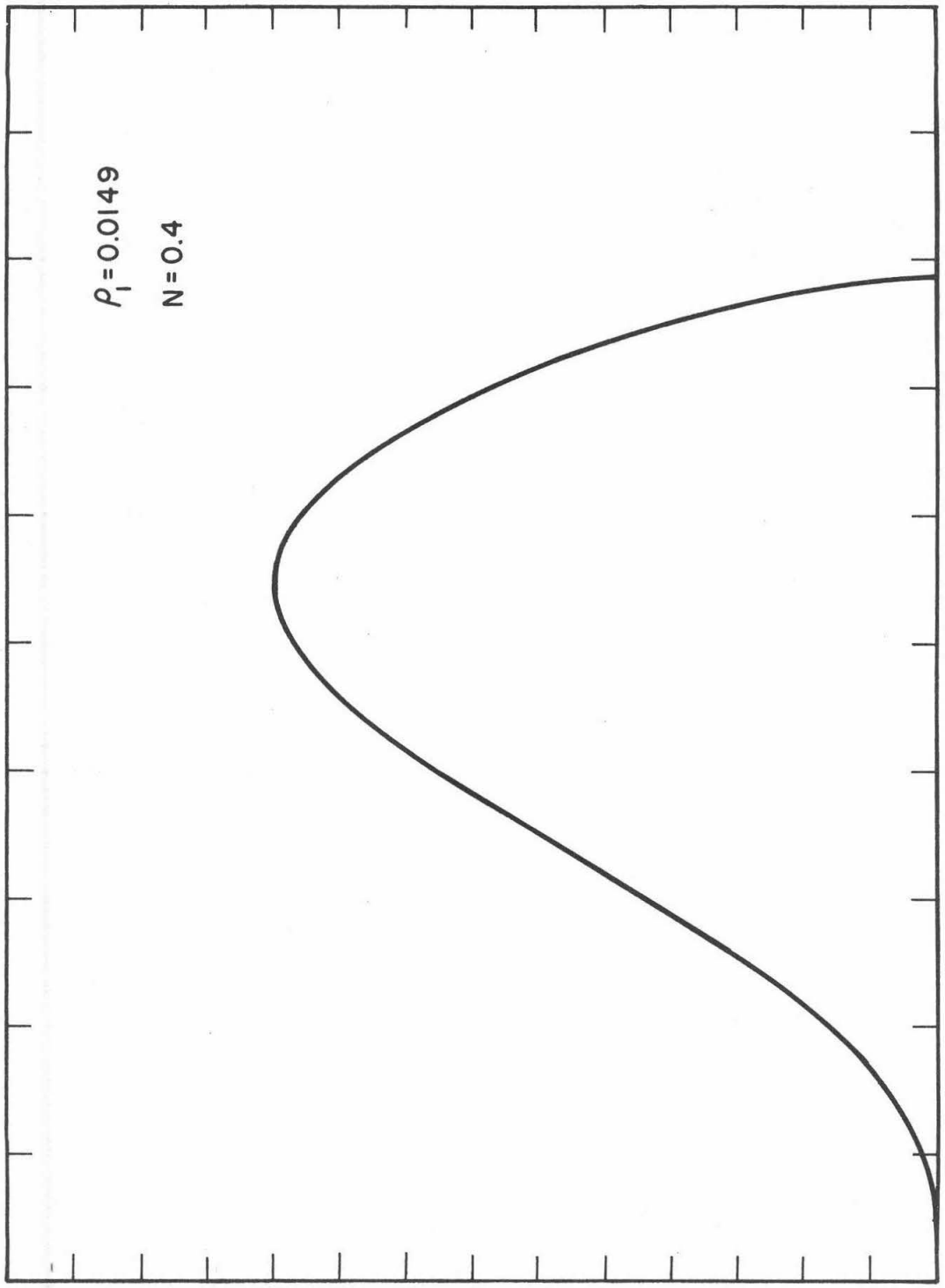

FIG. 5- CONTRIBUTION TO THE DENSITY PERTURBATION AS A FUNCTION OF THE APSIDAL ANGLE OF COLLISION (TERM LINEAR IN $(1-\rho_r)$)

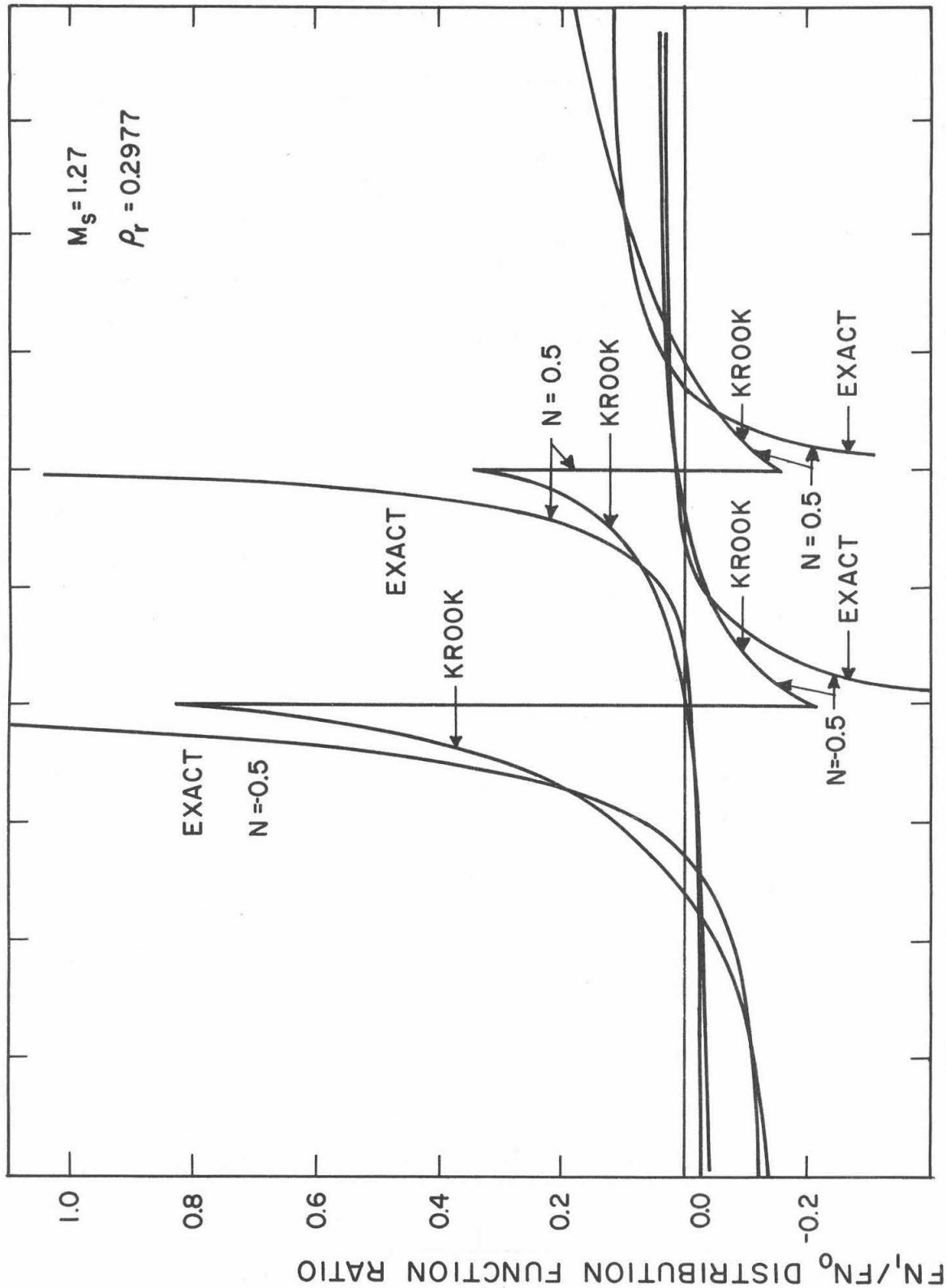

FIG. 6 - RATIO OF PERTURBATION TO COLLISIONLESS DISTRIBUTION FUNCTION

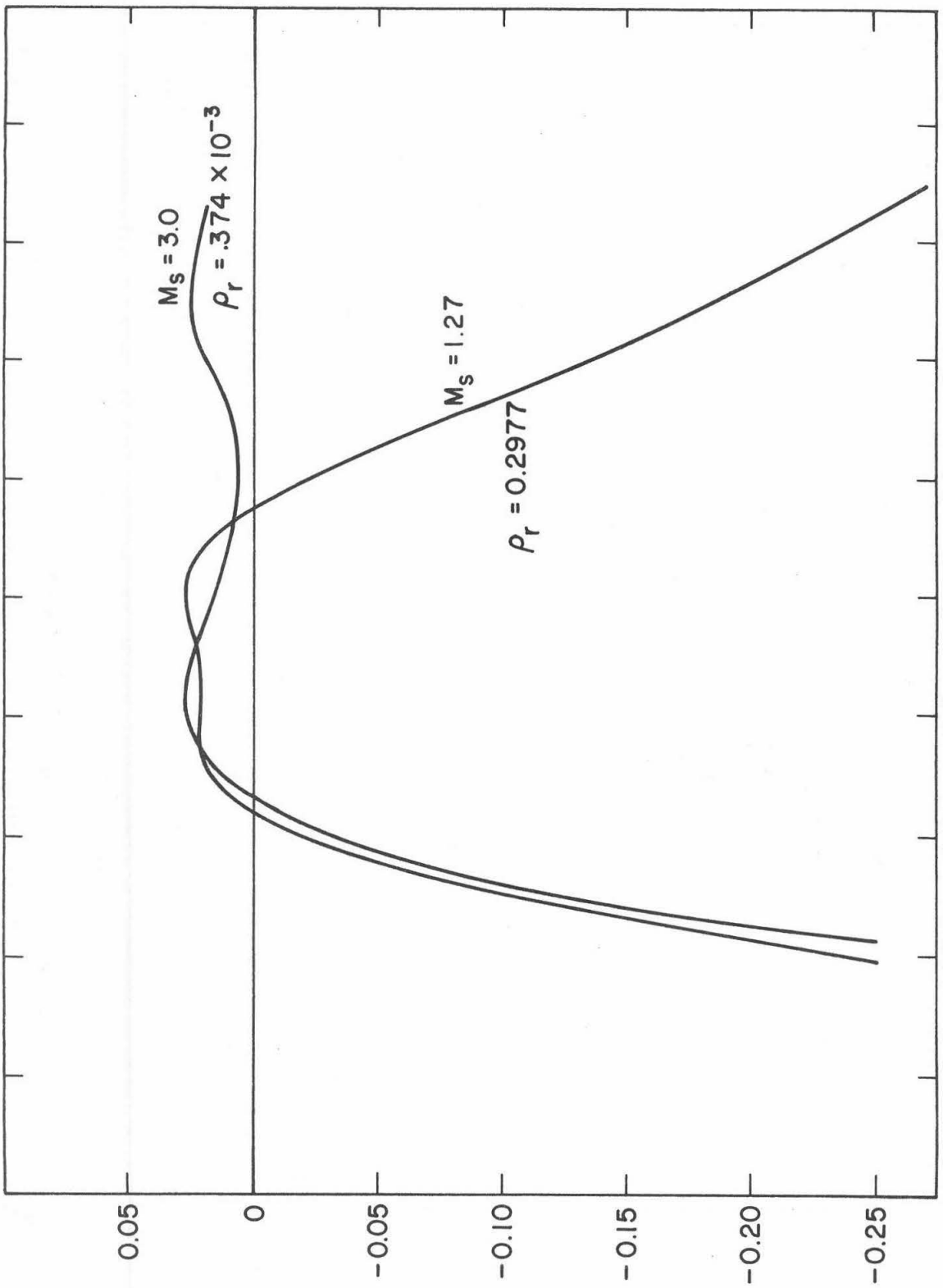

FIG. 7 - RATIO OF PERTURBATION TO COLLISIONLESS VELOCITY

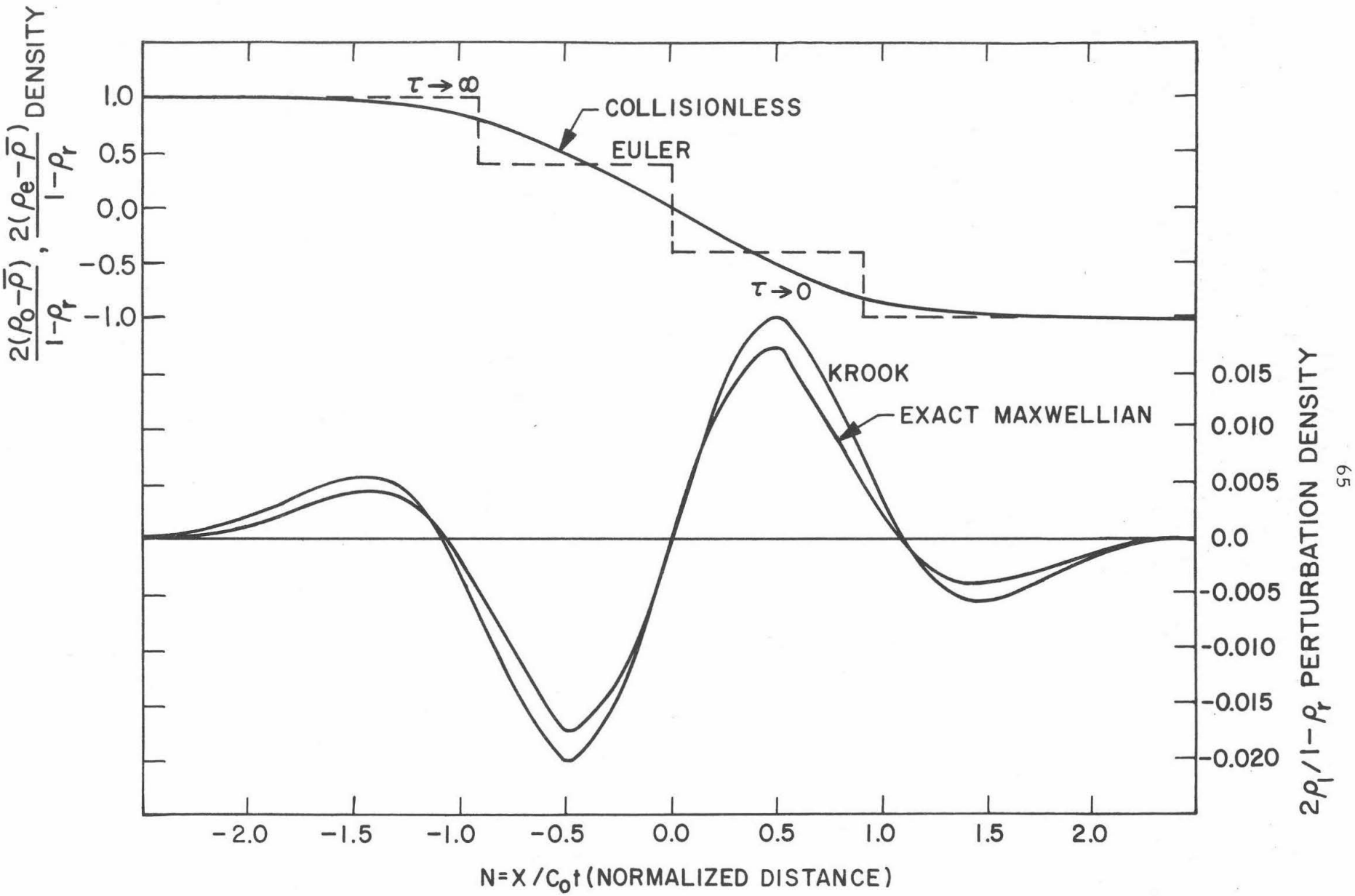

FIG. 8a - DENSITY PROFILES - LINEARIZED ($M_s = 1.00$, $\rho_r \to 1.00$)

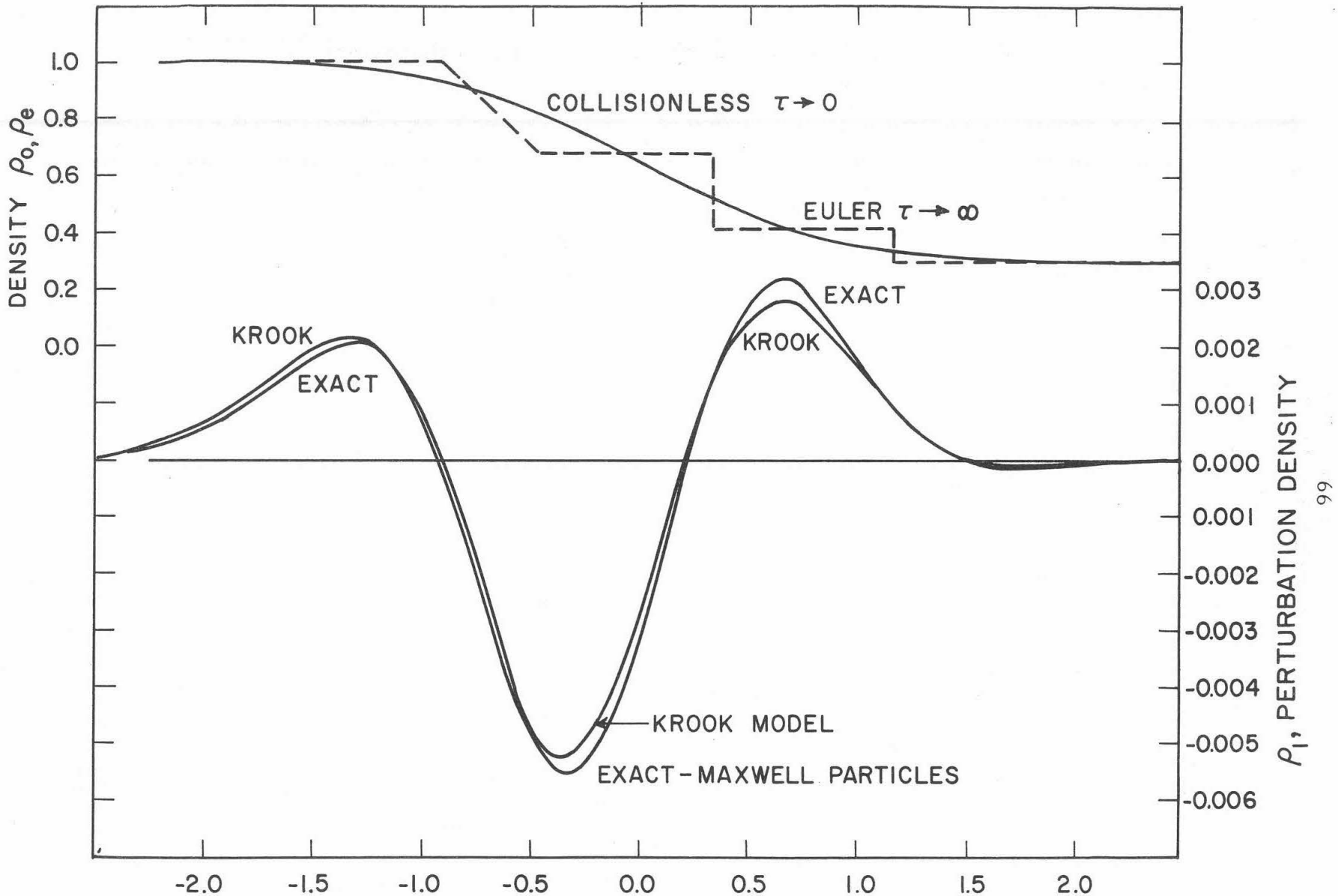

FIG. 8b - DENSITY PROFILES (M_s=1.27, ρ_r= 0.298)

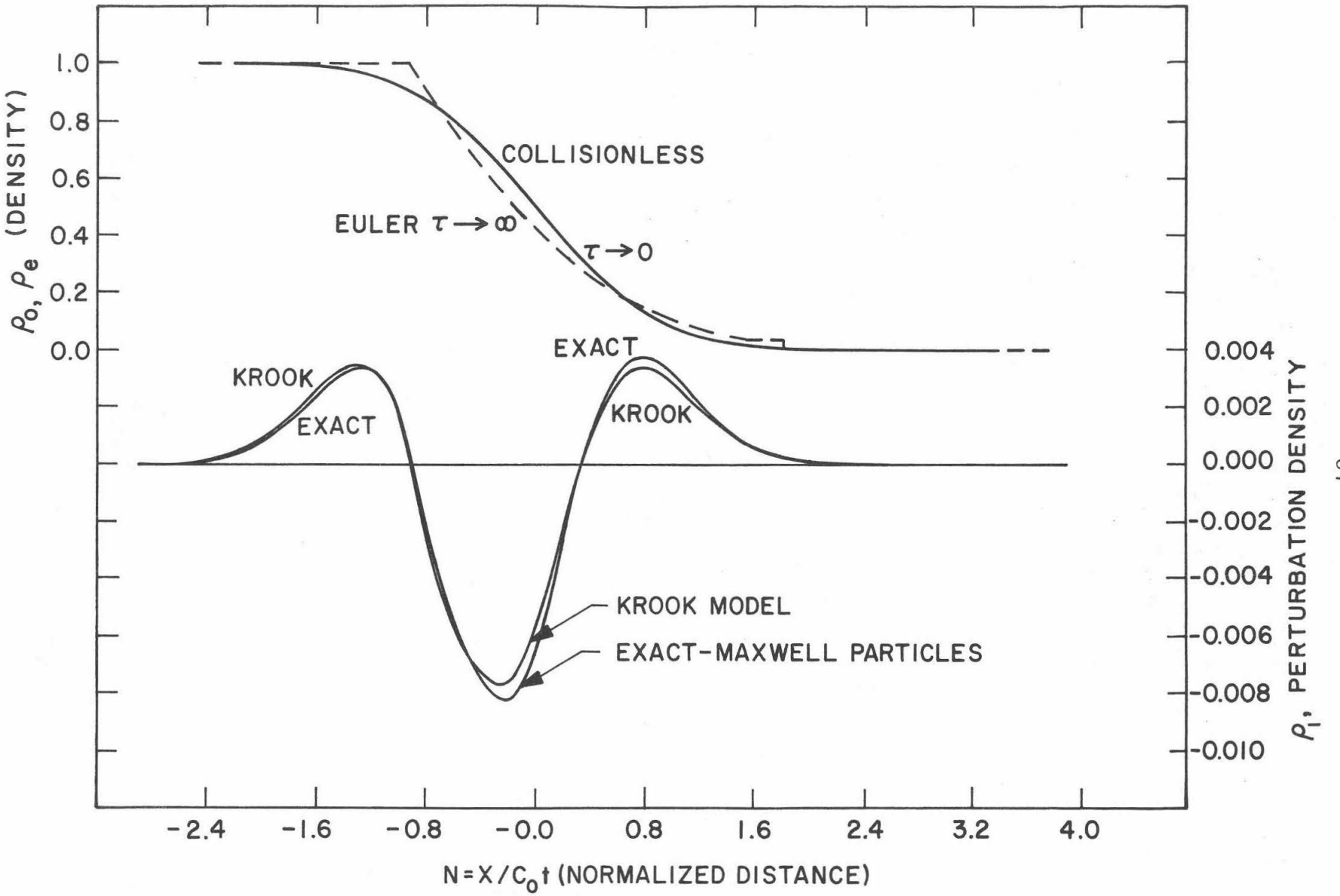

FIG 8c—DENSITY PROFILES ($M_s = 3.00$, $\rho_r = 0.375 \times 10^{-3}$)

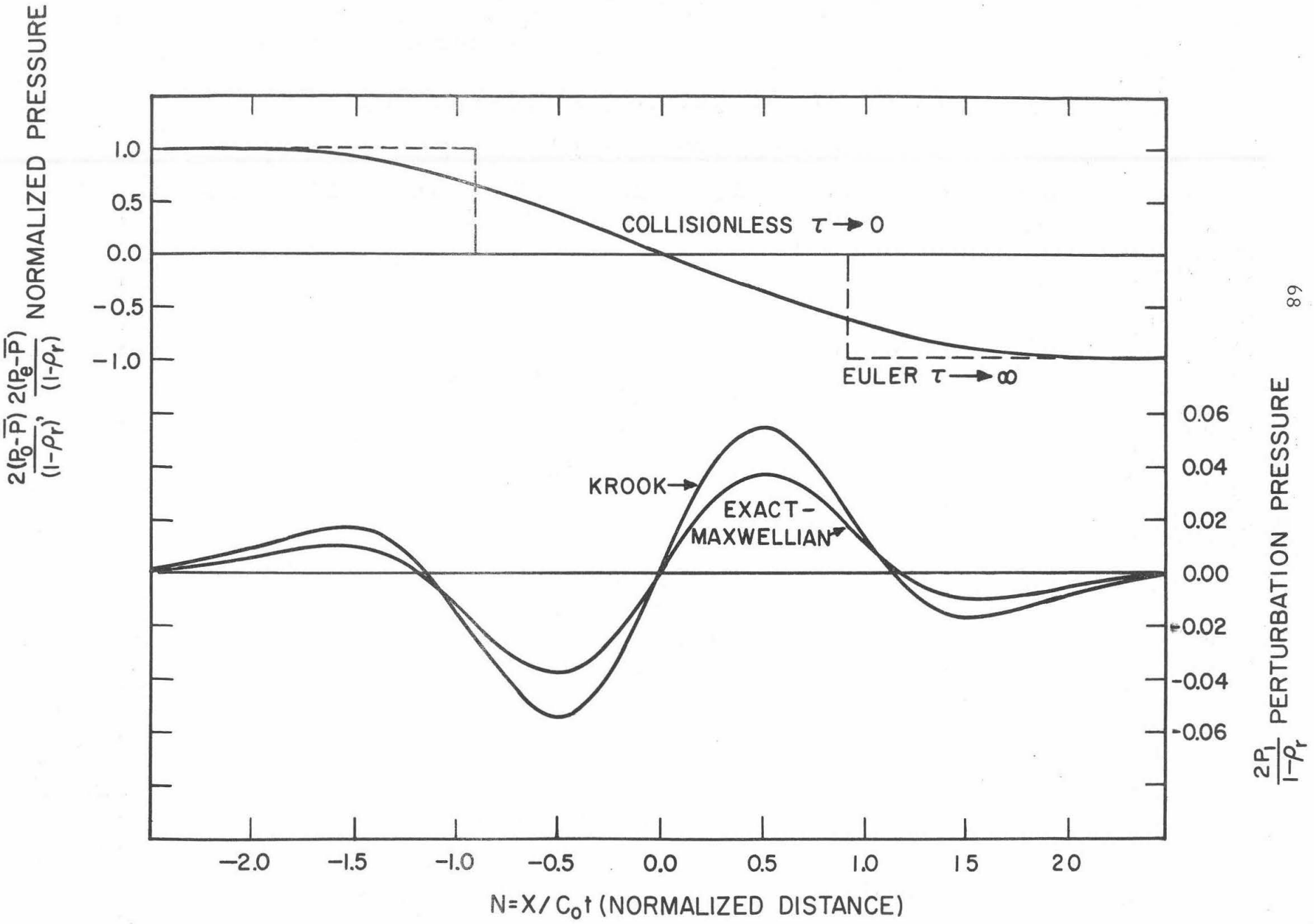

Fig. 9a PRESSURE PROFILE - LINEARIZED ($M_s = 1.00, \rho_r \to 1.00$)

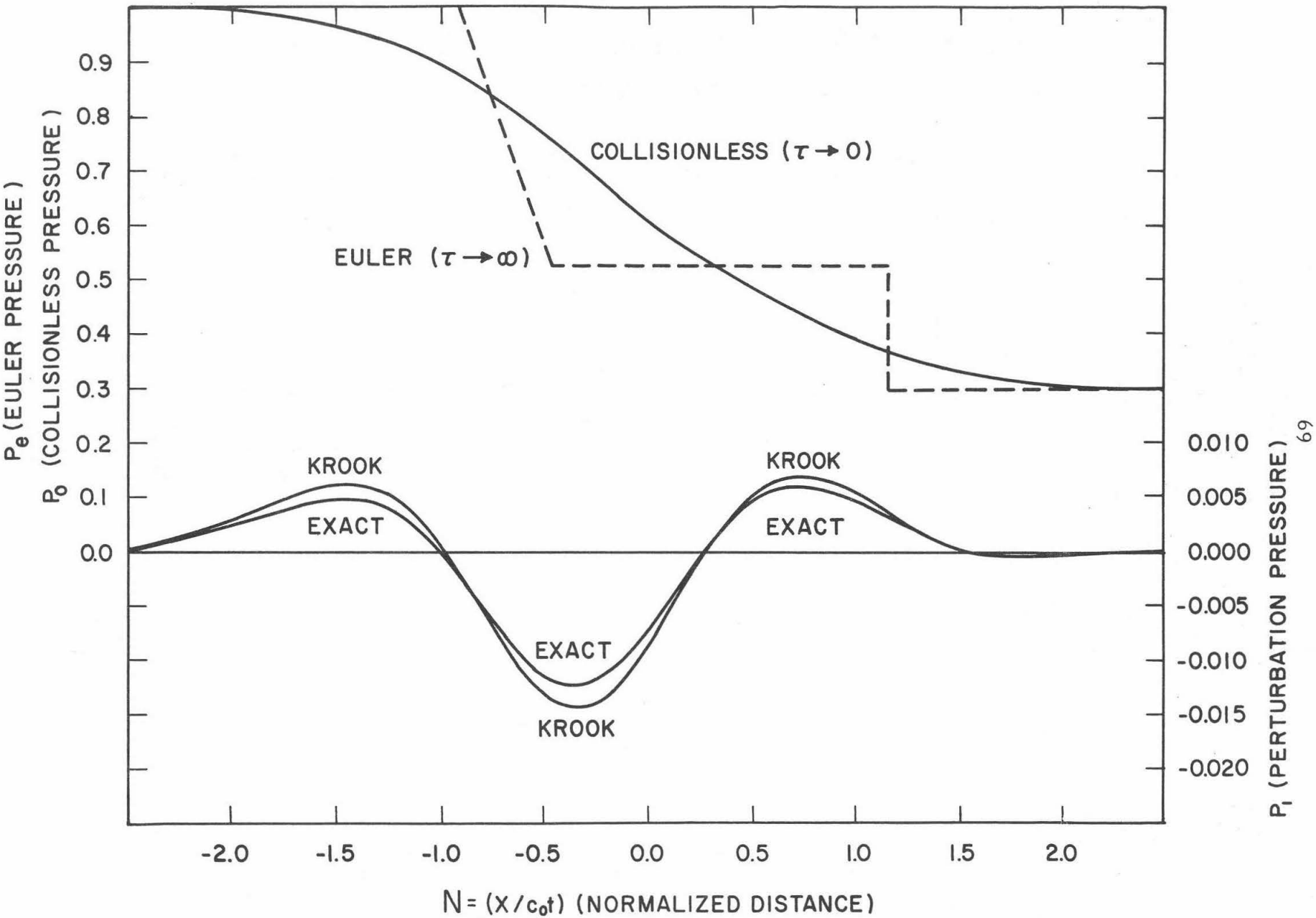

FIG. 9b – PRESSURE PROFILES (M_s=1.27, ρ_r=0.298)

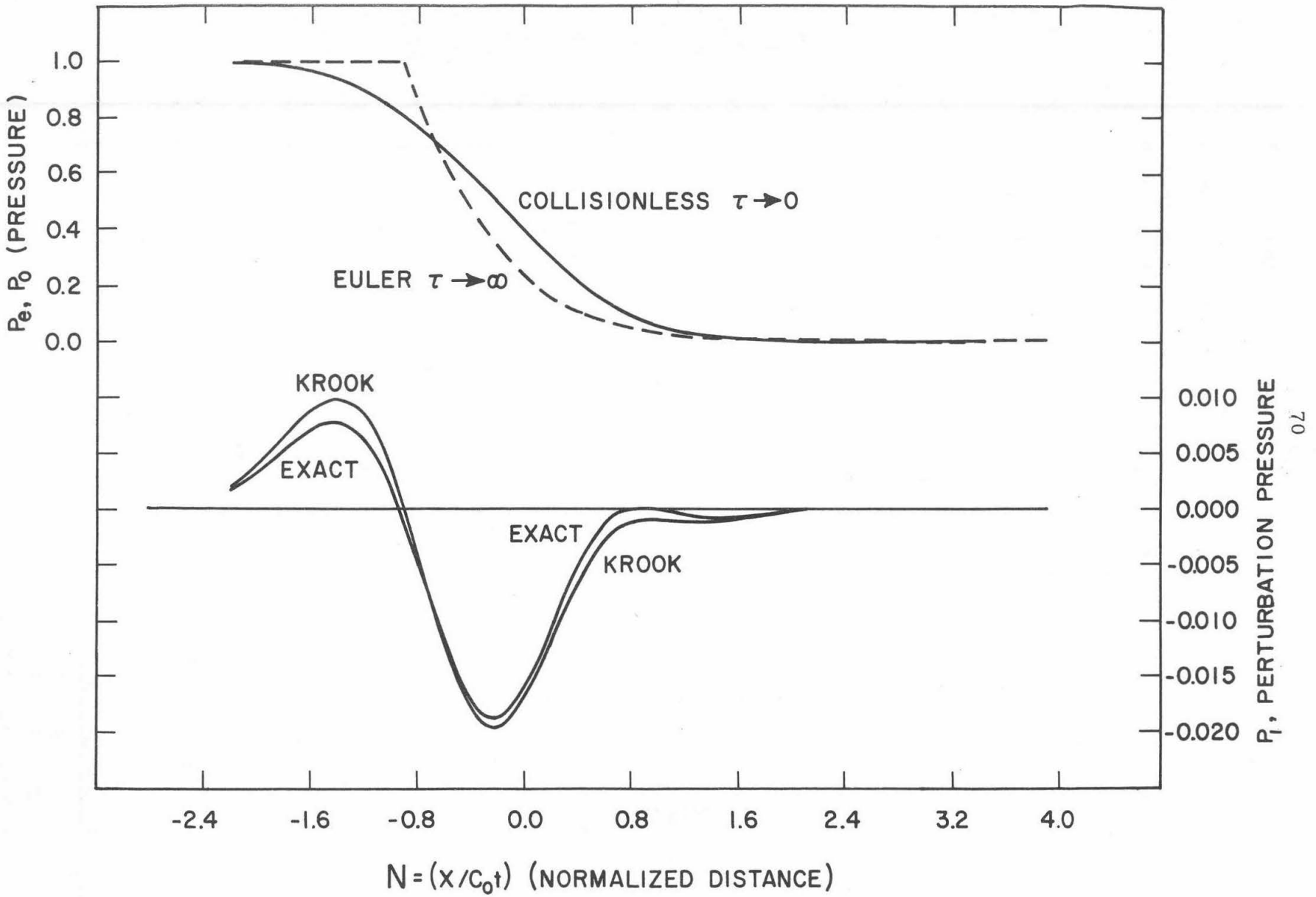

FIG. 9c – PRESSURE PROFILES (M_s=3.00, $\rho_r = 0.375 \times 10^{-3}$)

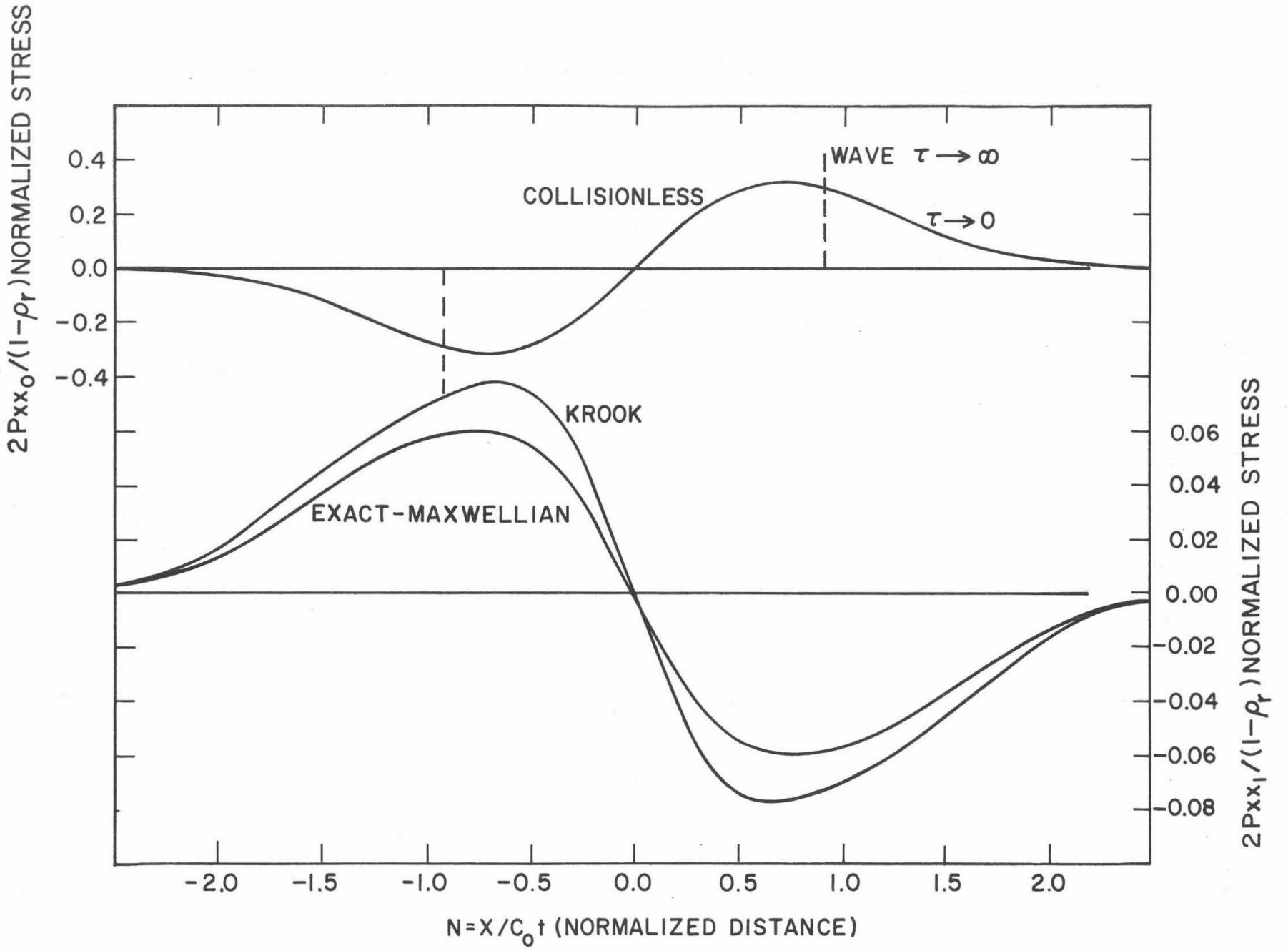

FIG. 10a - STRESS PROFILES - LINEARIZED ($M_s = 1.00$, $\rho_r \to 1.00$)

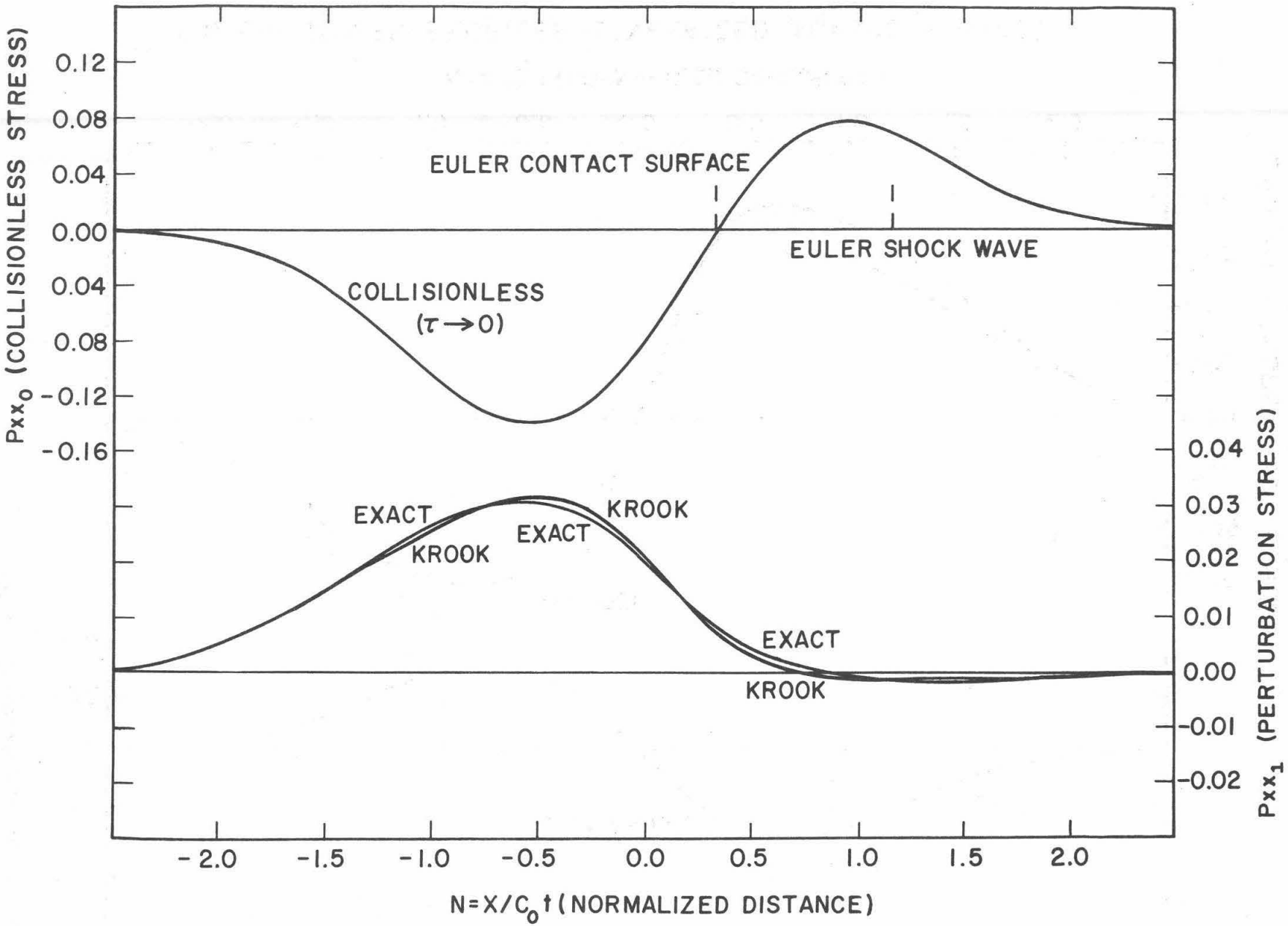

FIG.10b - STRESS PROFILES ($M_s = 1.27$, $\rho_r = 0.298$)

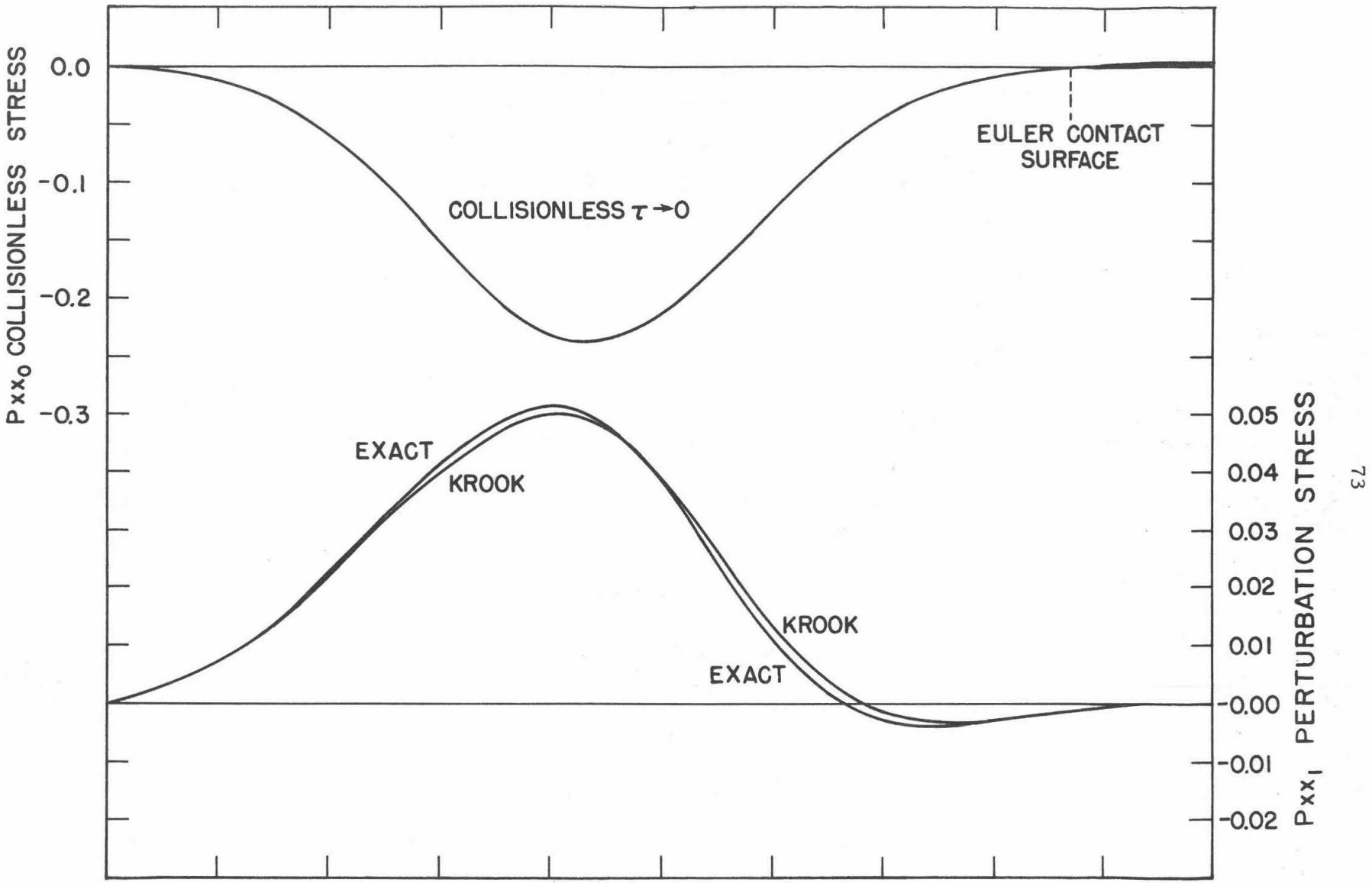

FIG. 10c – STRESS PROFILES ($M_S = 3.00, \rho_r = 0.375 \times 10^{-3}$)

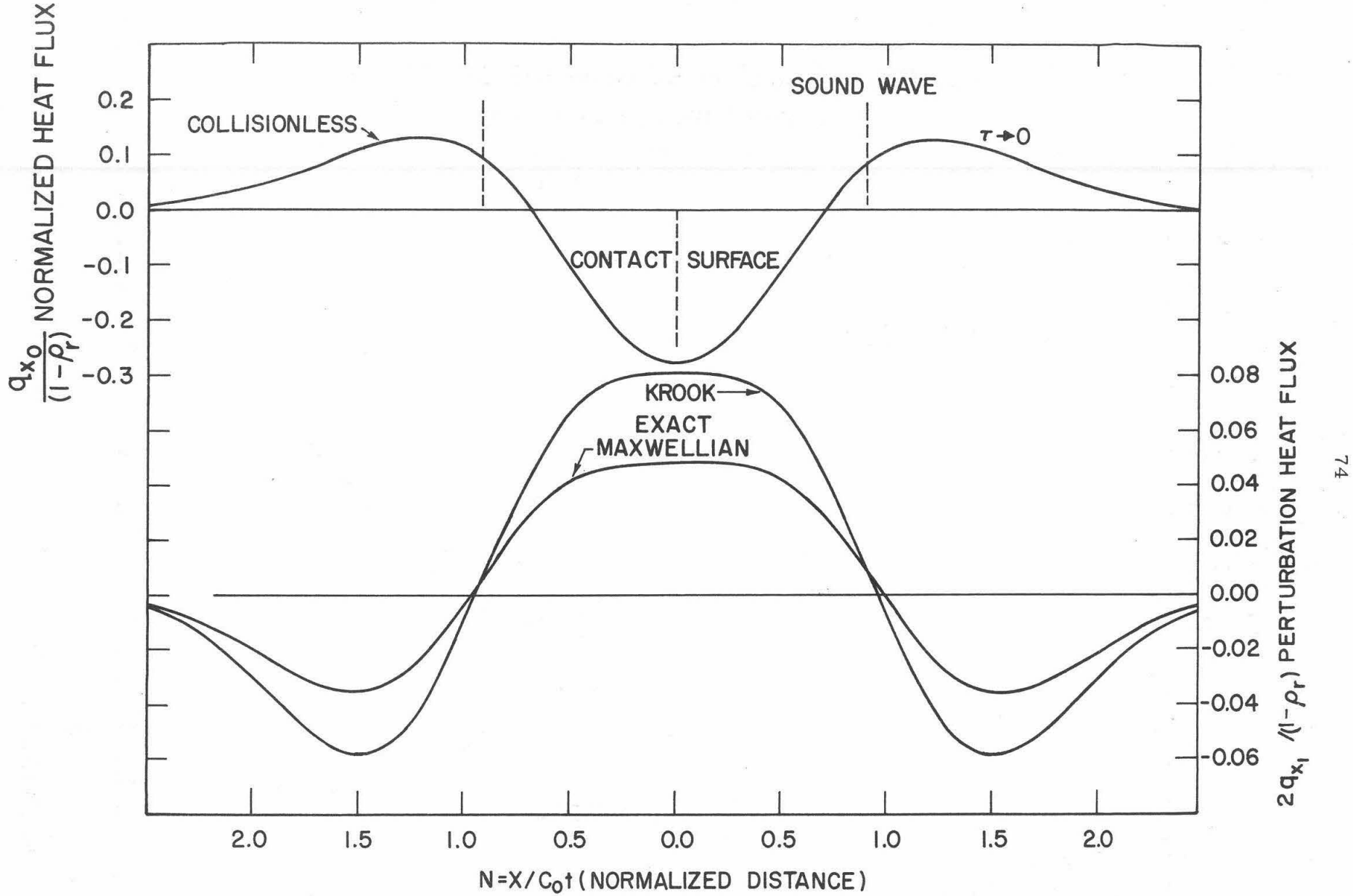

FIG. 11a — HEAT FLUX PROFILES — LINEARIZED (M_s= 1.00, $\rho_r \to$ 1.00)

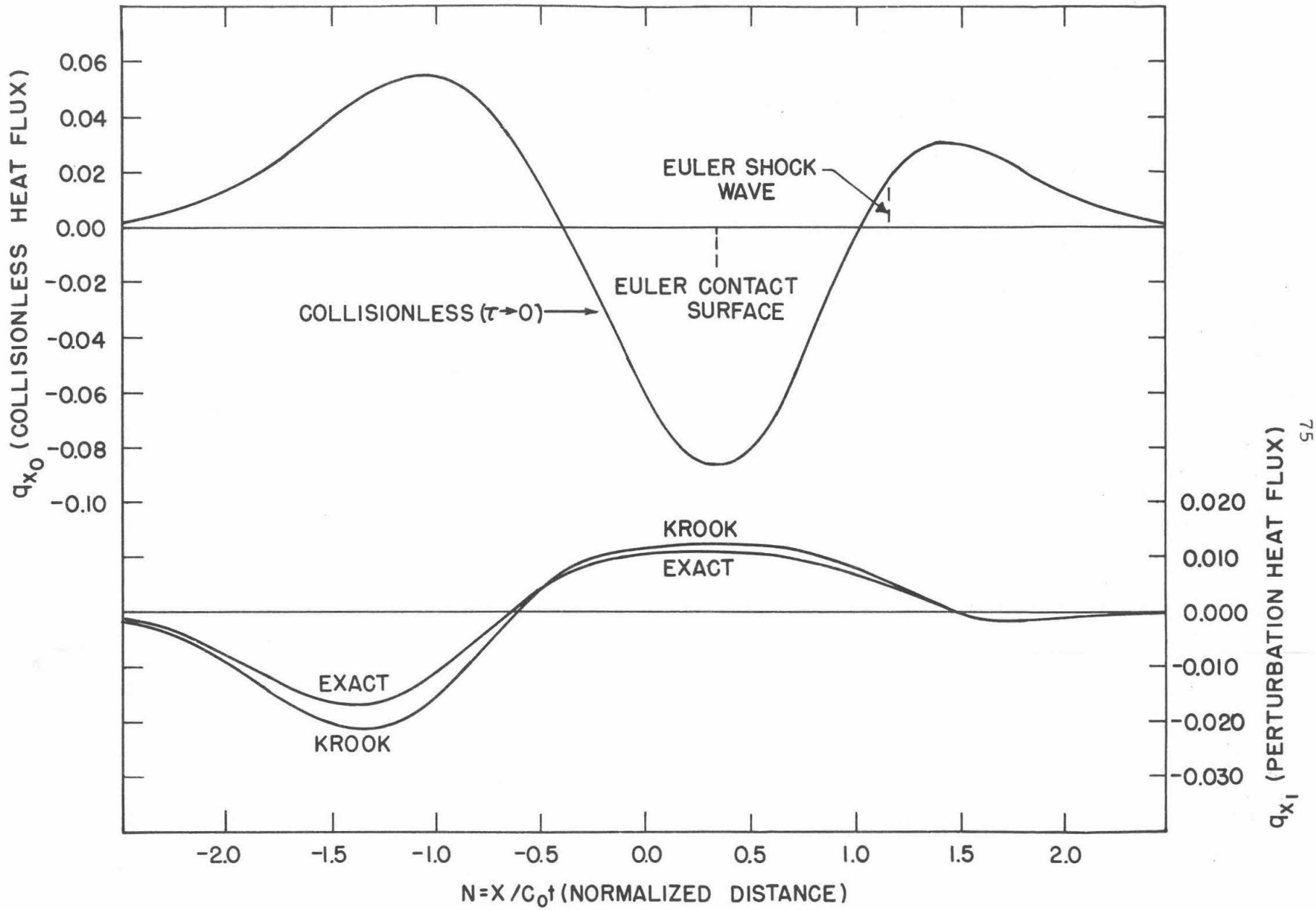

FIG. 11b — HEAT FLUX PROFILES (M_S = 1.27, ρ_r = 0.298)

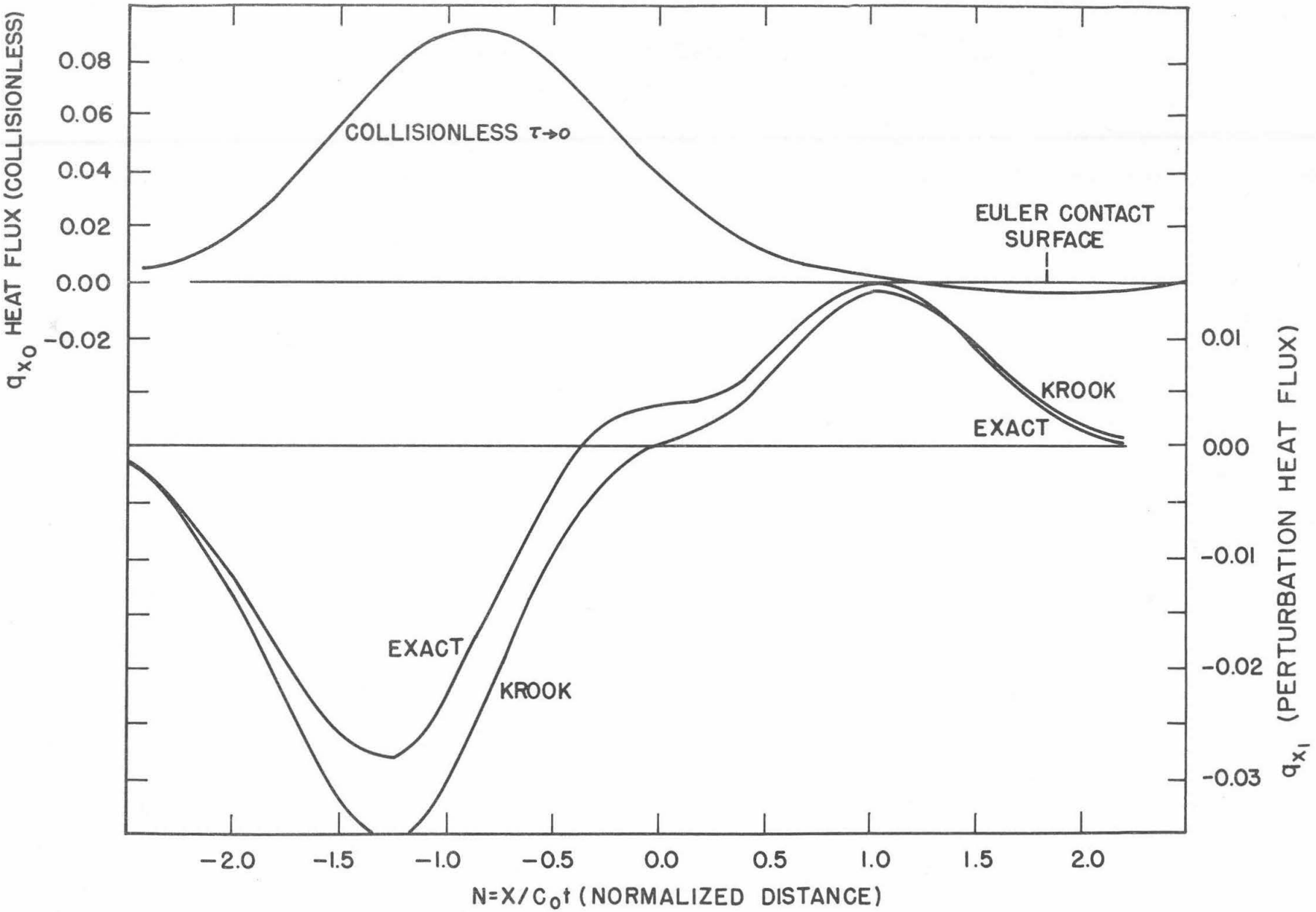

FIG. IIc —HEAT FLUX PROFILES (M_s=3.00,ρ_r=0.375X10^{-3})

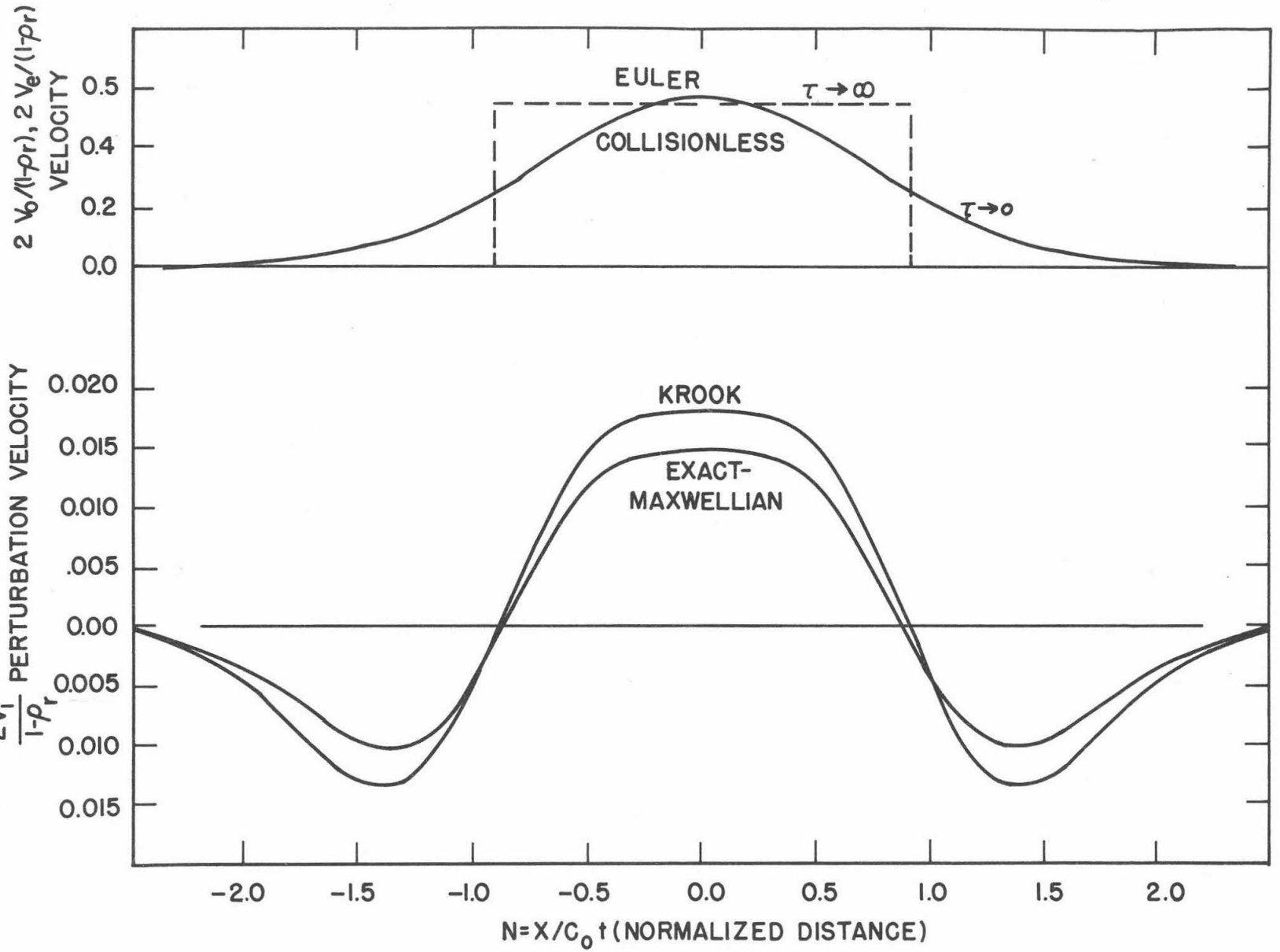

FIG. 12a—VELOCITY PROFILES—LINEARIZED (M_s=1.00, $\rho_r \rightarrow$1.00)

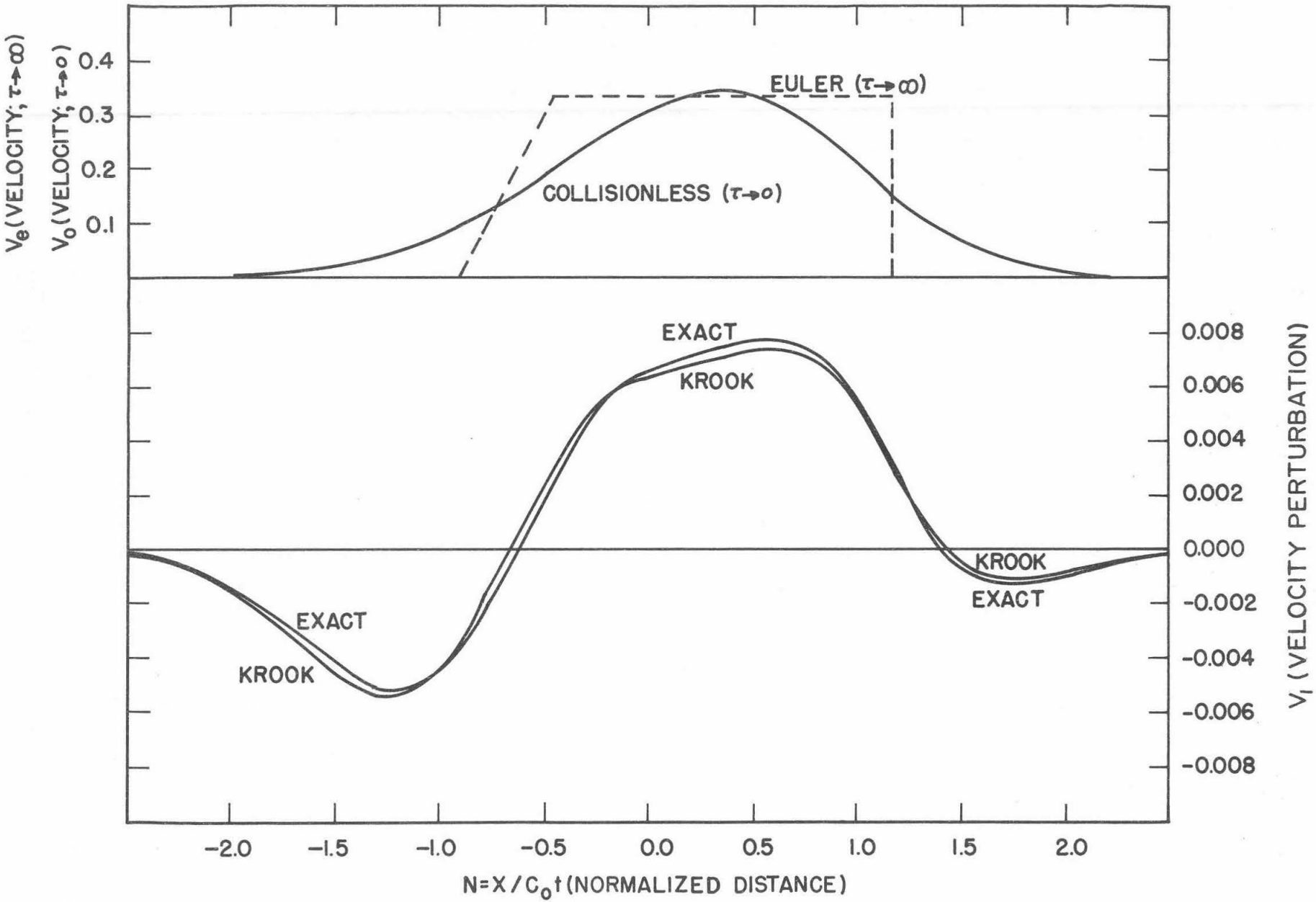

FIG. 12b– VELOCITY PROFILES (M_s=1.27,ρ_r=0.298)

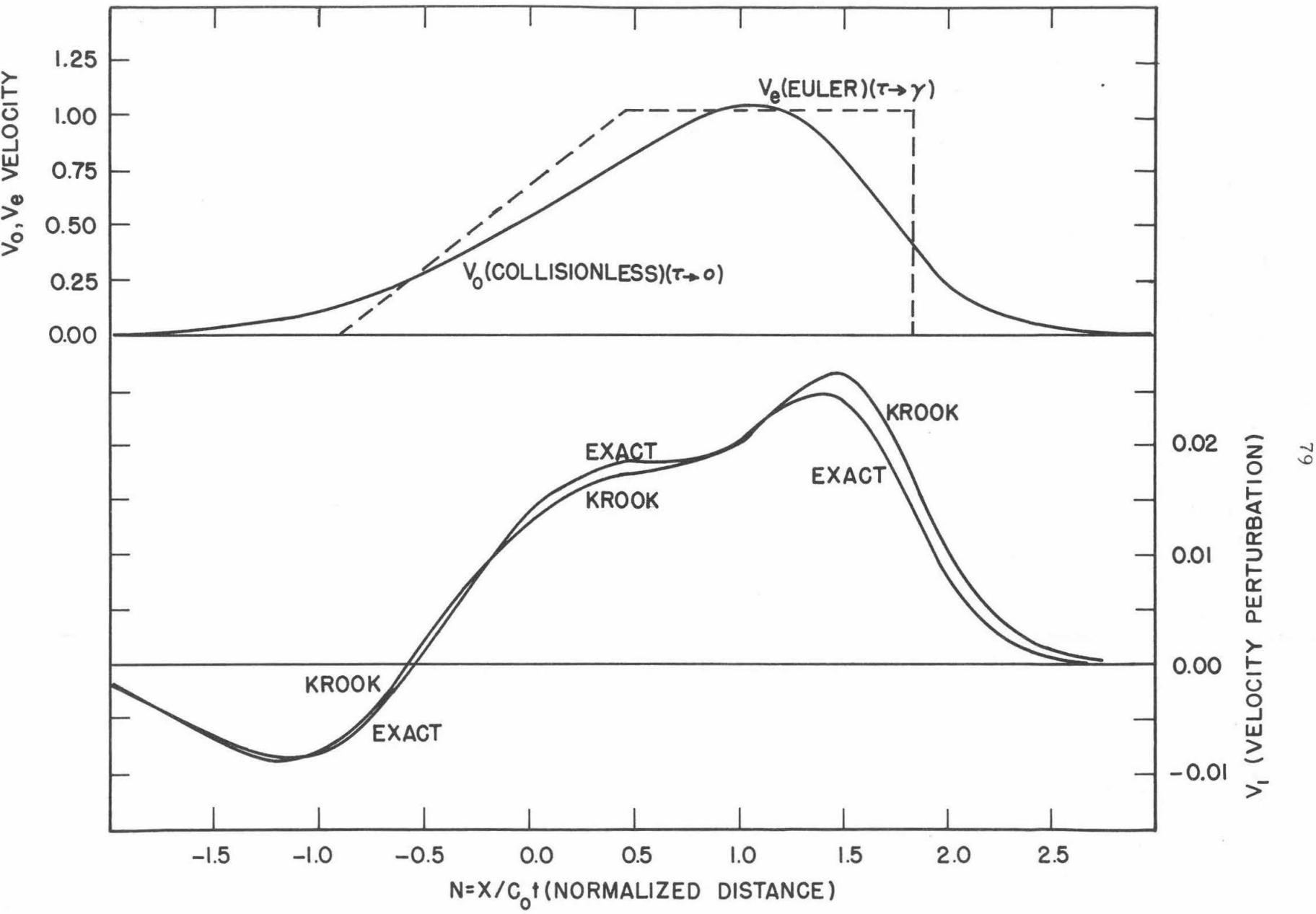

FIG. 12c — VELOCITY PROFILES (M_s = 2.00, ρ_r=0.201X10^{-1})

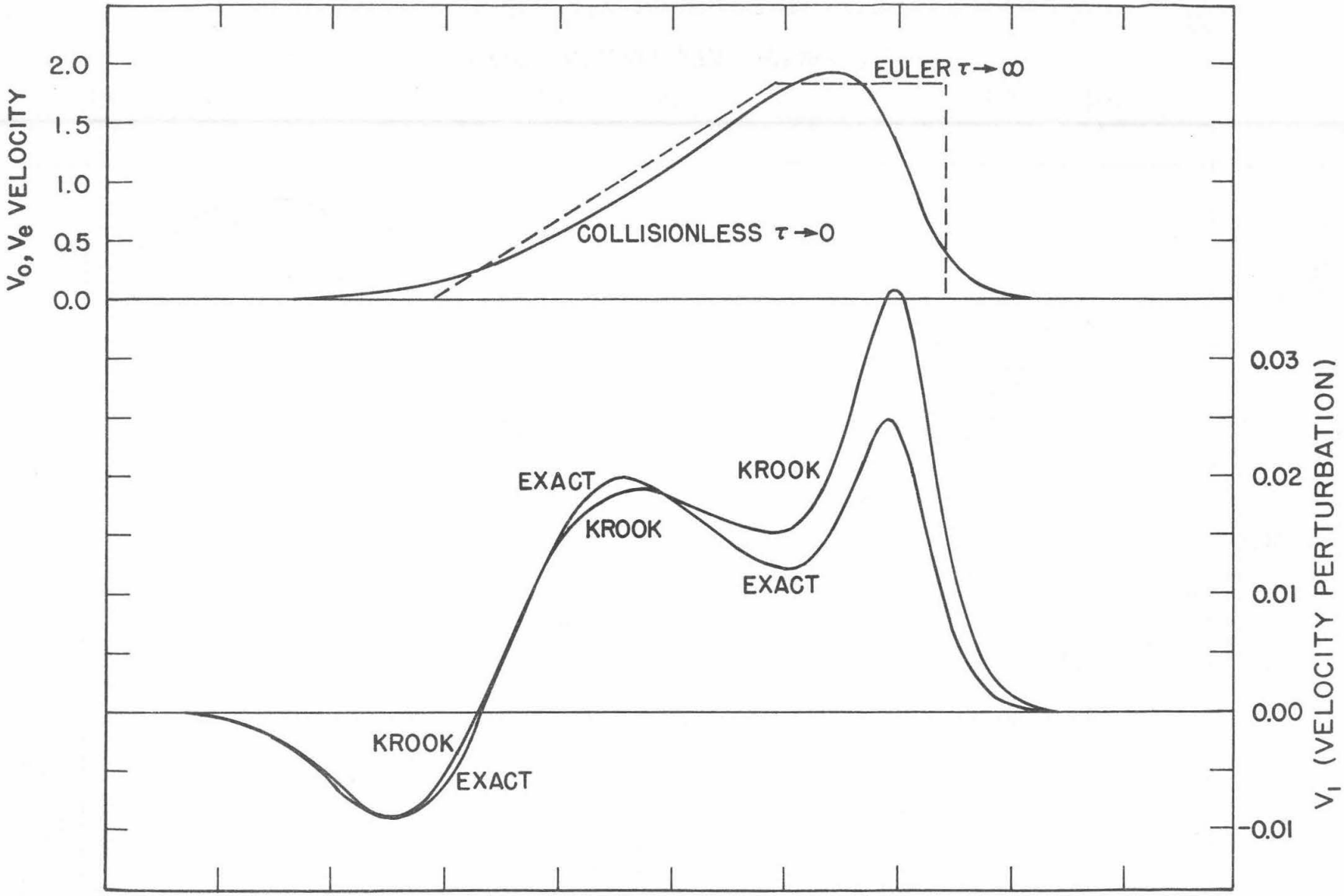

FIG. 12d – VELOCITY PROFILES ($M_S = 3.00, \rho_r = 0.375 \times 10^{-3}$)

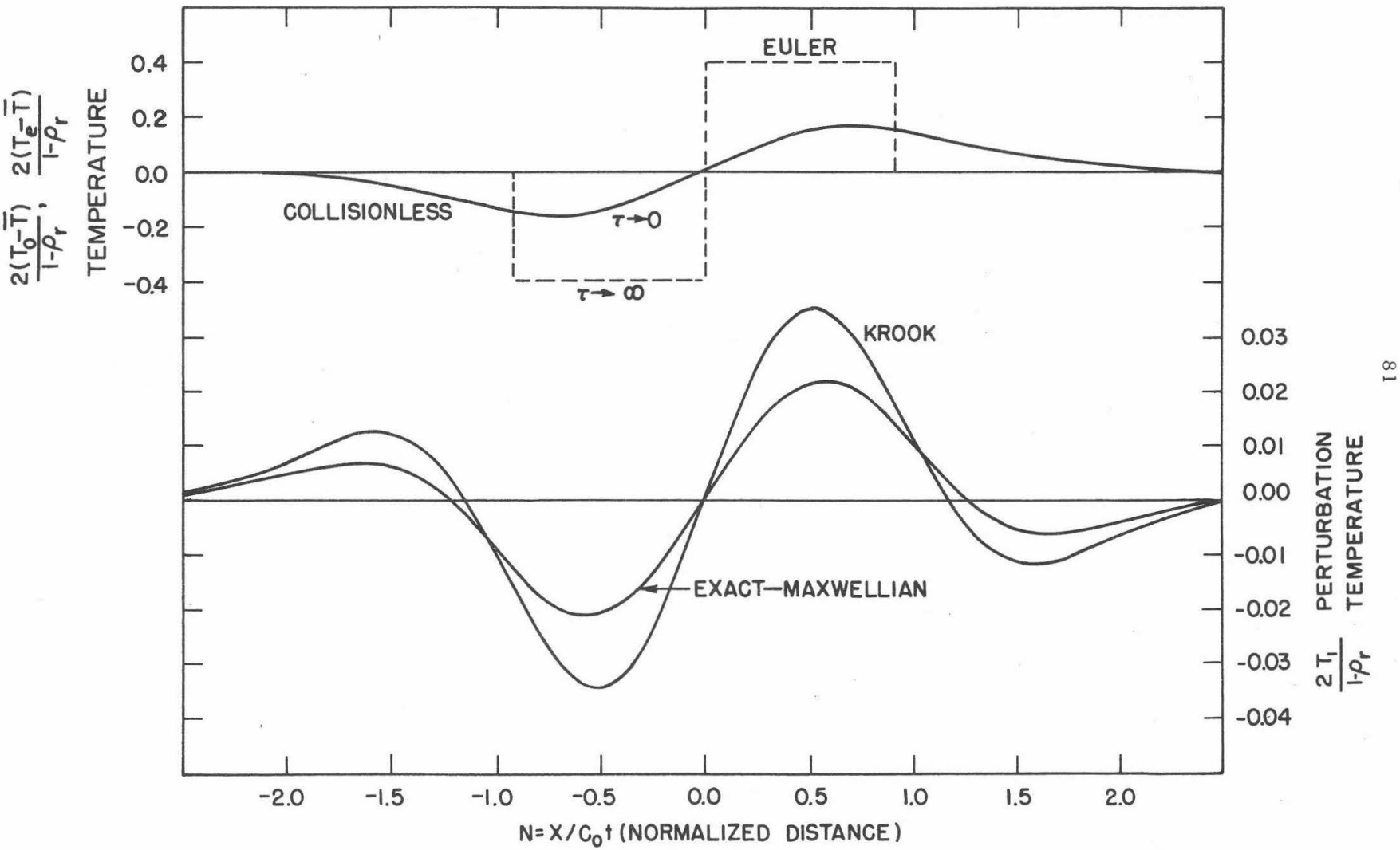

FIG. 13a – TEMPERATURE PROFILES - LINEARIZED (M_S=1.00, $\rho_r \rightarrow$ 1.00)

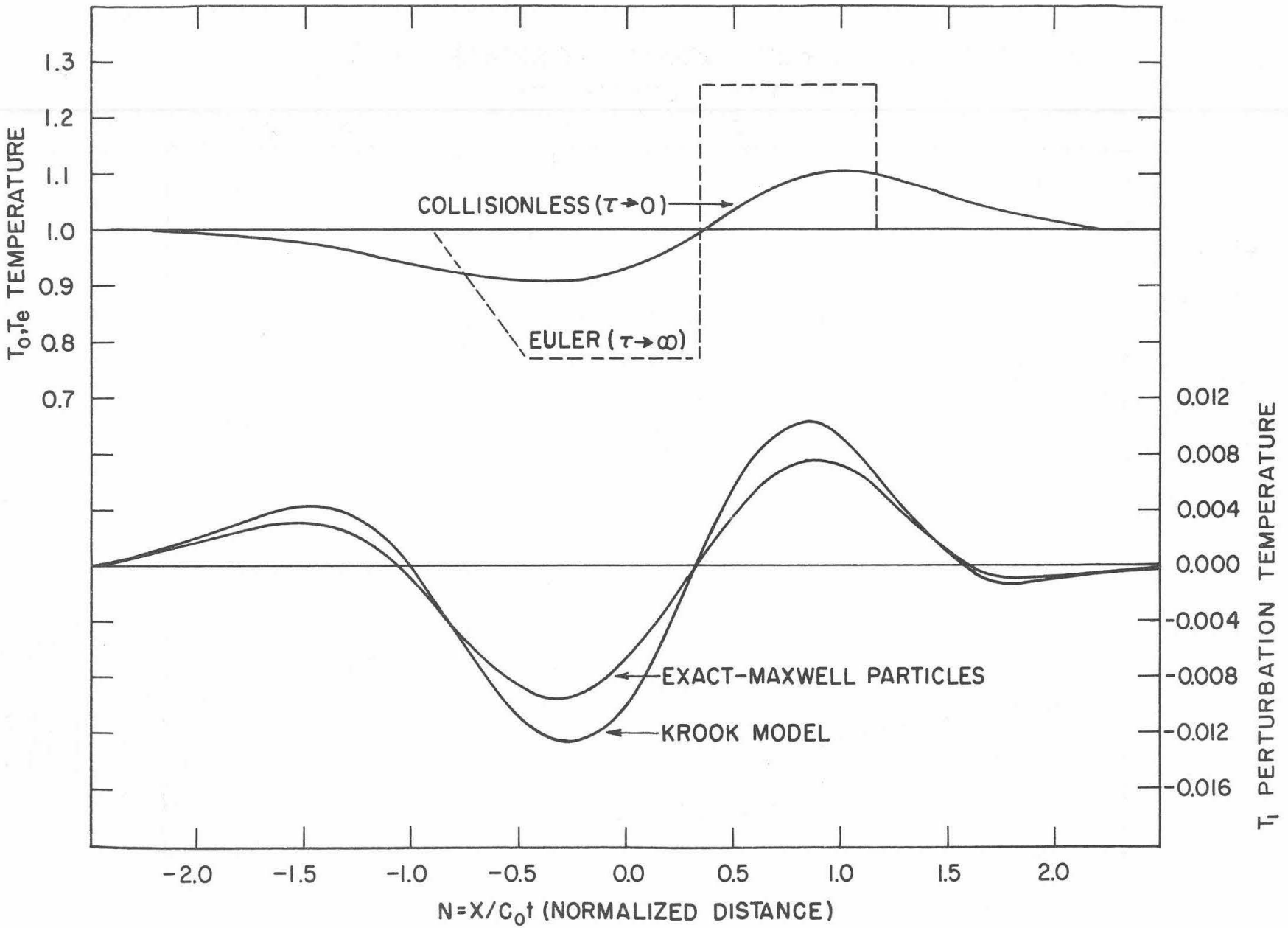

FIG. 13b - TEMPERATURE PROFILES ($M_s = 1.27, \rho_r = 0.298$)

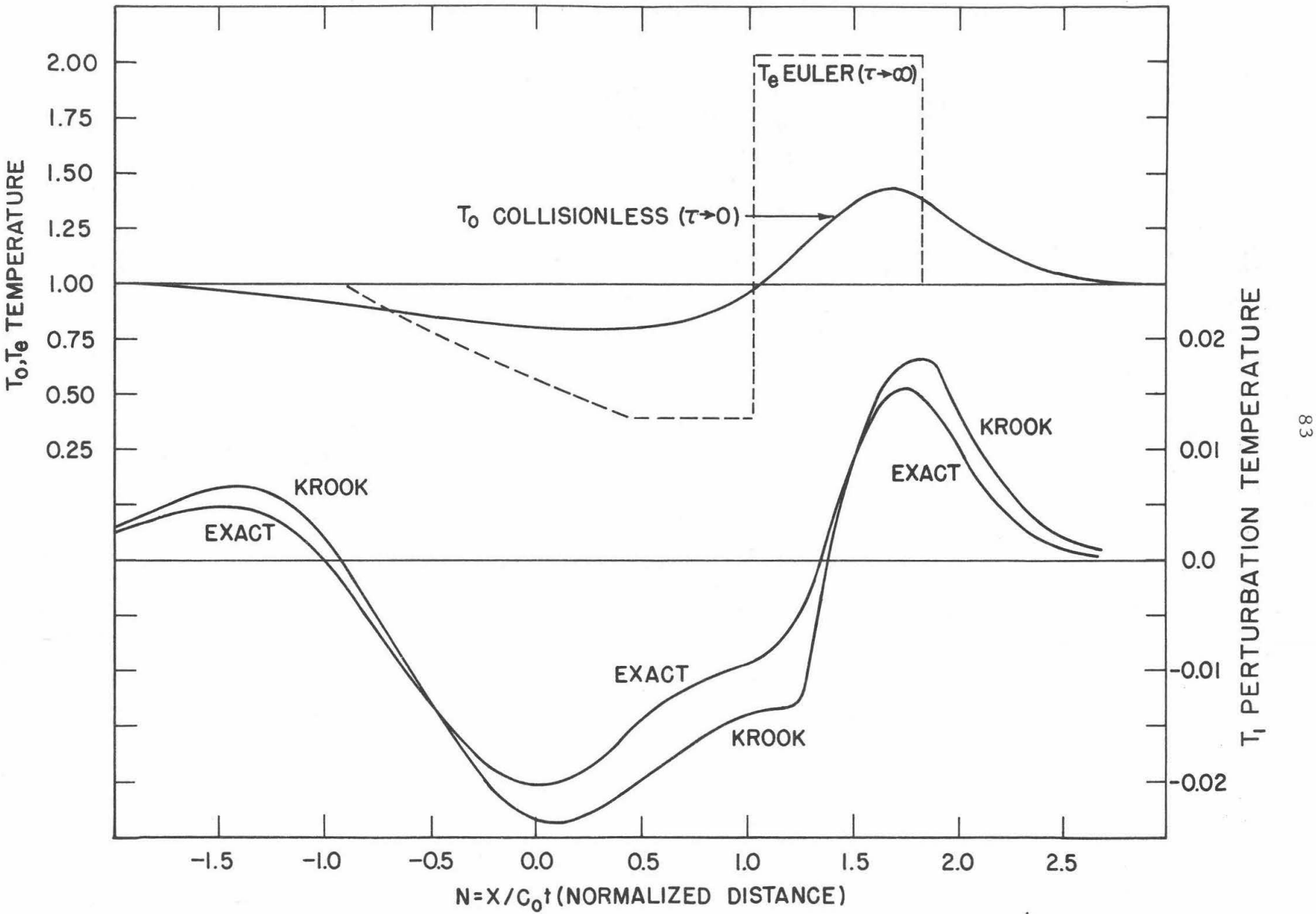

FIG. 13c – TEMPERATURE PROFILES ($M_S = 2.00, \rho_r = 0.201 \times 10^{-1}$)

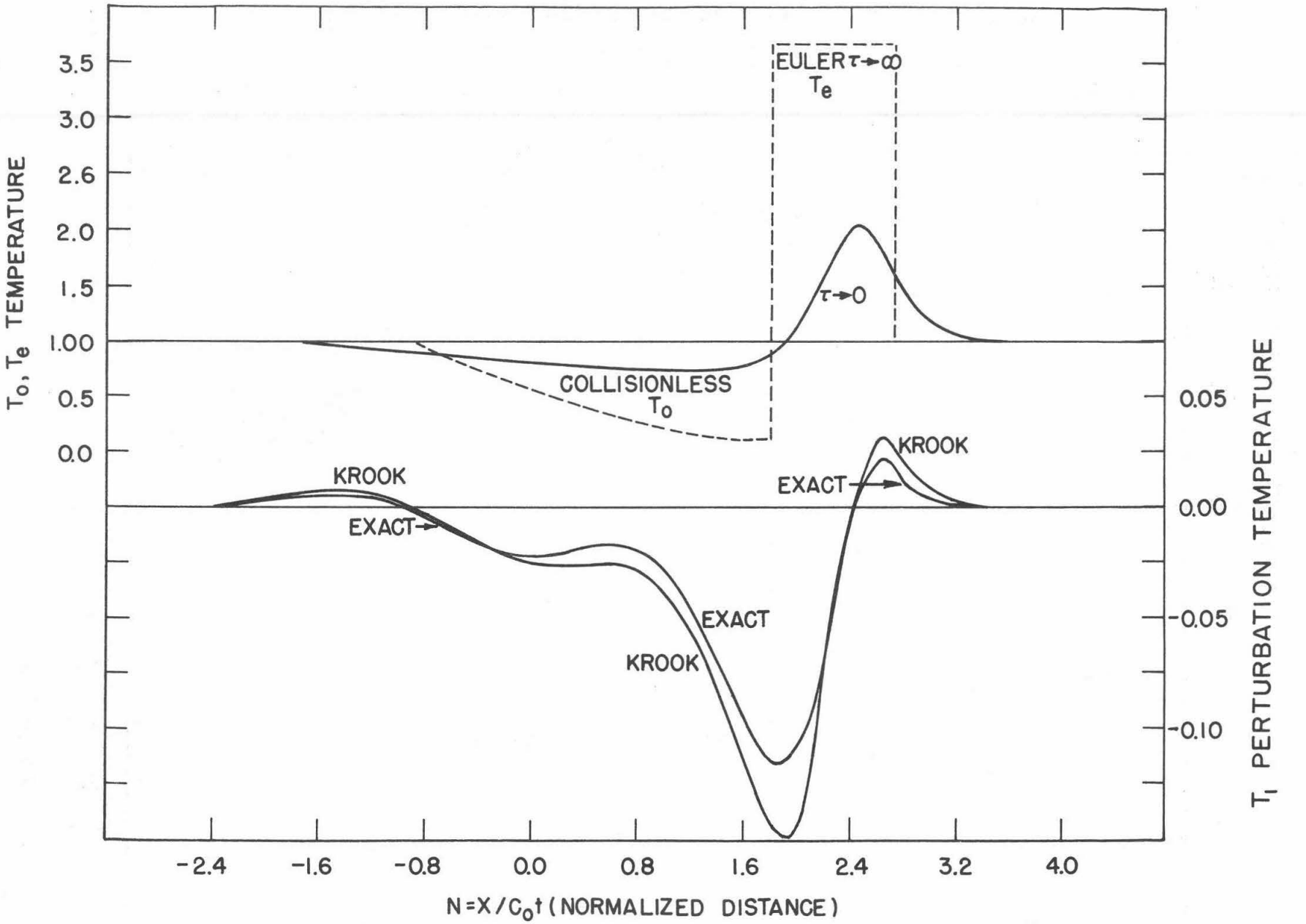

FIG. 13d – TEMPERATURE PROFILES ($M_s = 3.00, \rho_r = 0.375 \times 10^{-3}$)

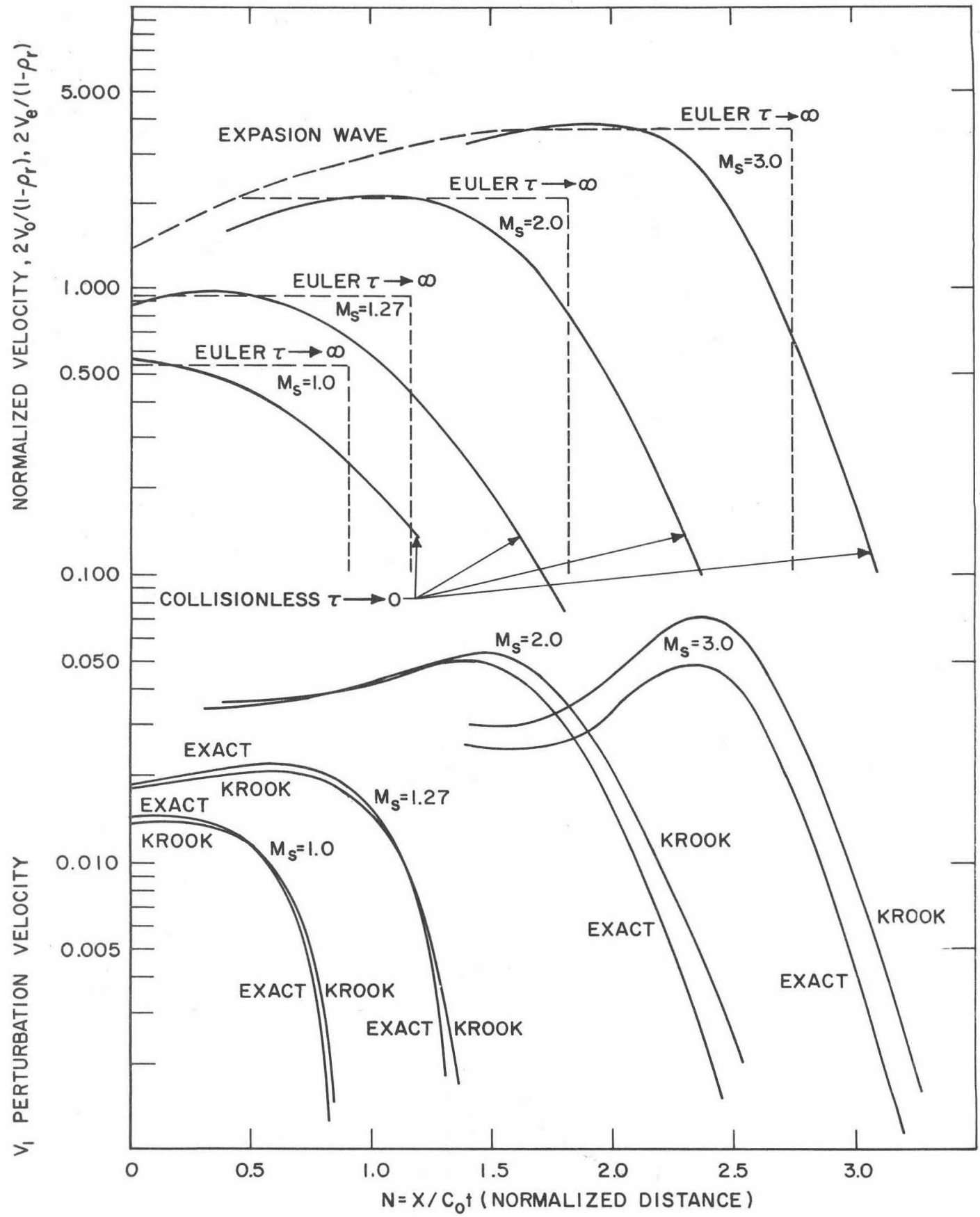

FIG. 14–SUMMARY OF VELOCITY PROFILES

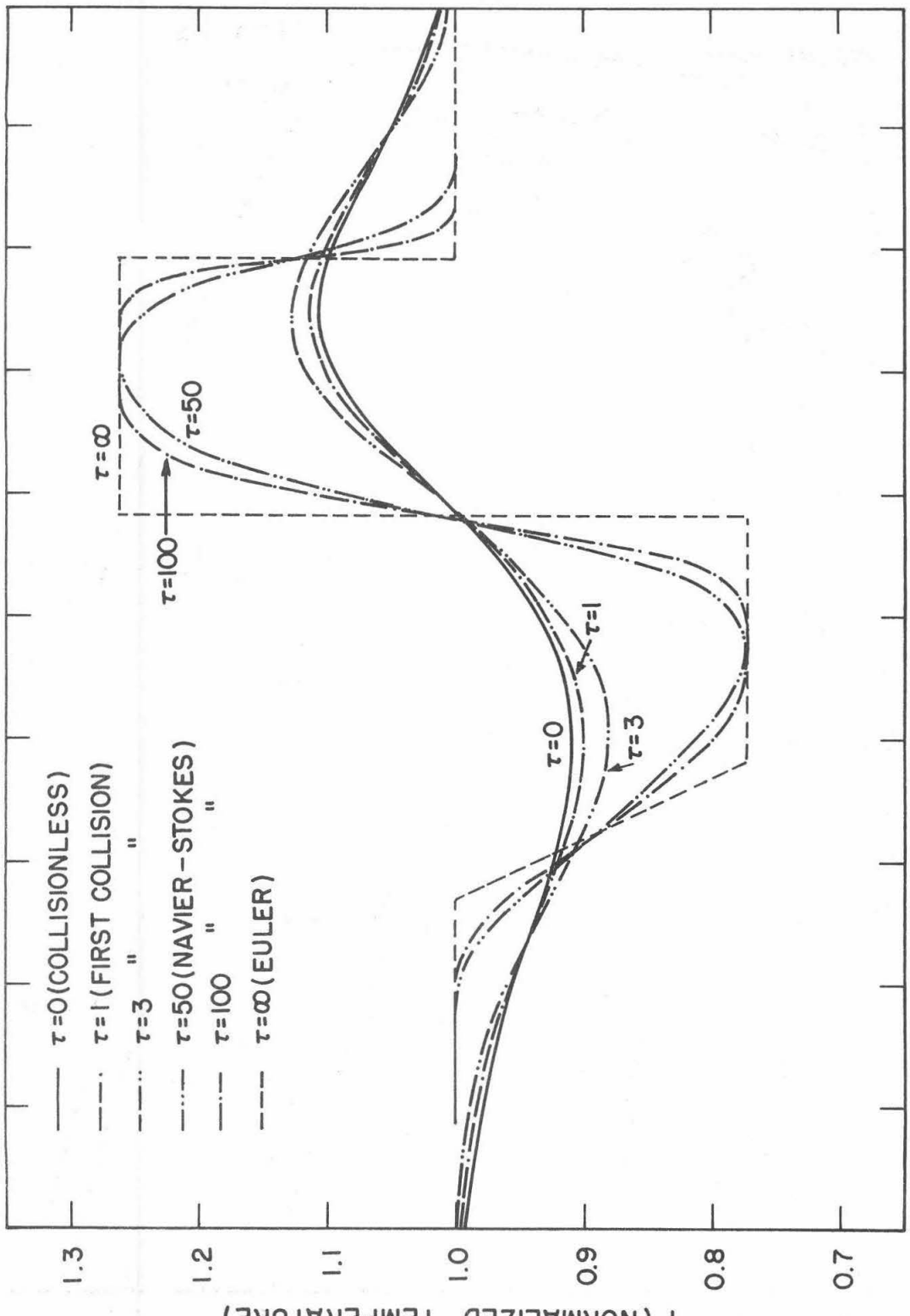

FIG.15 TEMPERATURE PROFILES AT SEVERAL TIMES (M_S= 1.27, ρ_r = 0.298)

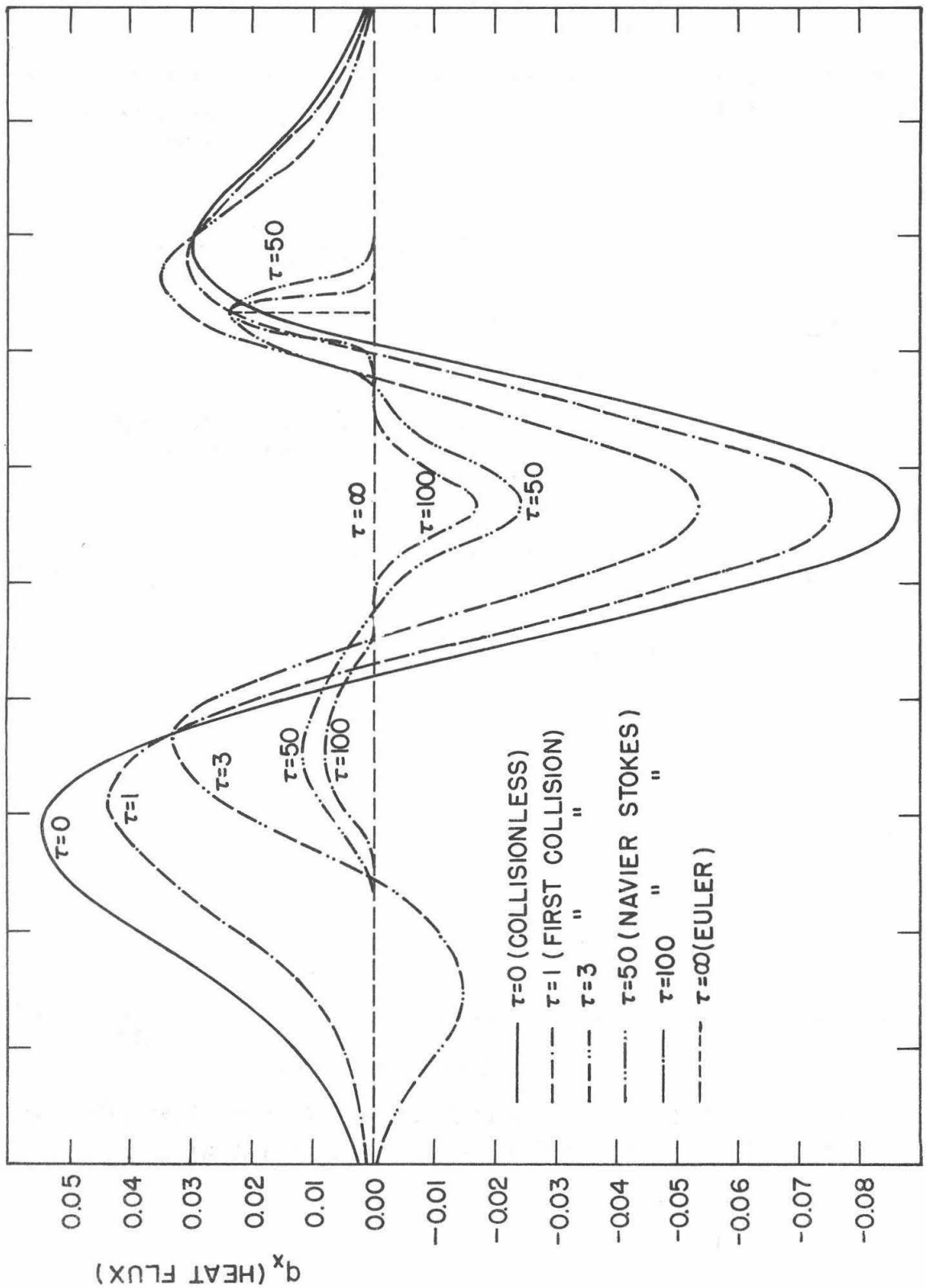

FIG. 16-HEAT FLUX PROFILES AT SEVERAL TIMES (M_s= 1.27, ρ_r =0.298)

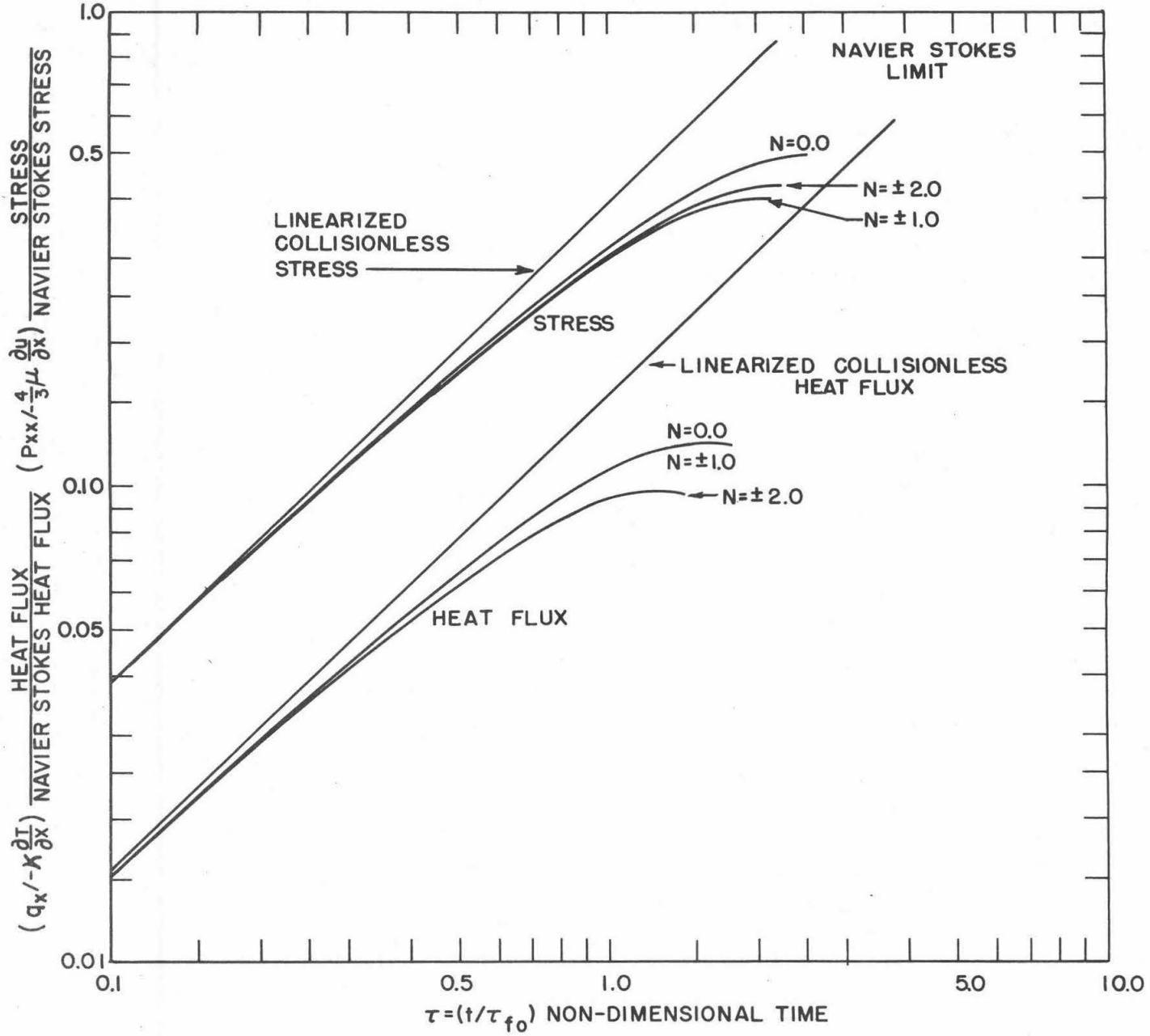

FIG. 17 - STRESS - STRAIN RATE RATIO AND HEAT FLUX - TEMPERATURE GRADIENT RATIO VS. TIME - LINEARIZED (M_s = 1.00, $\rho_{\bar{r}} \to 1.00$)

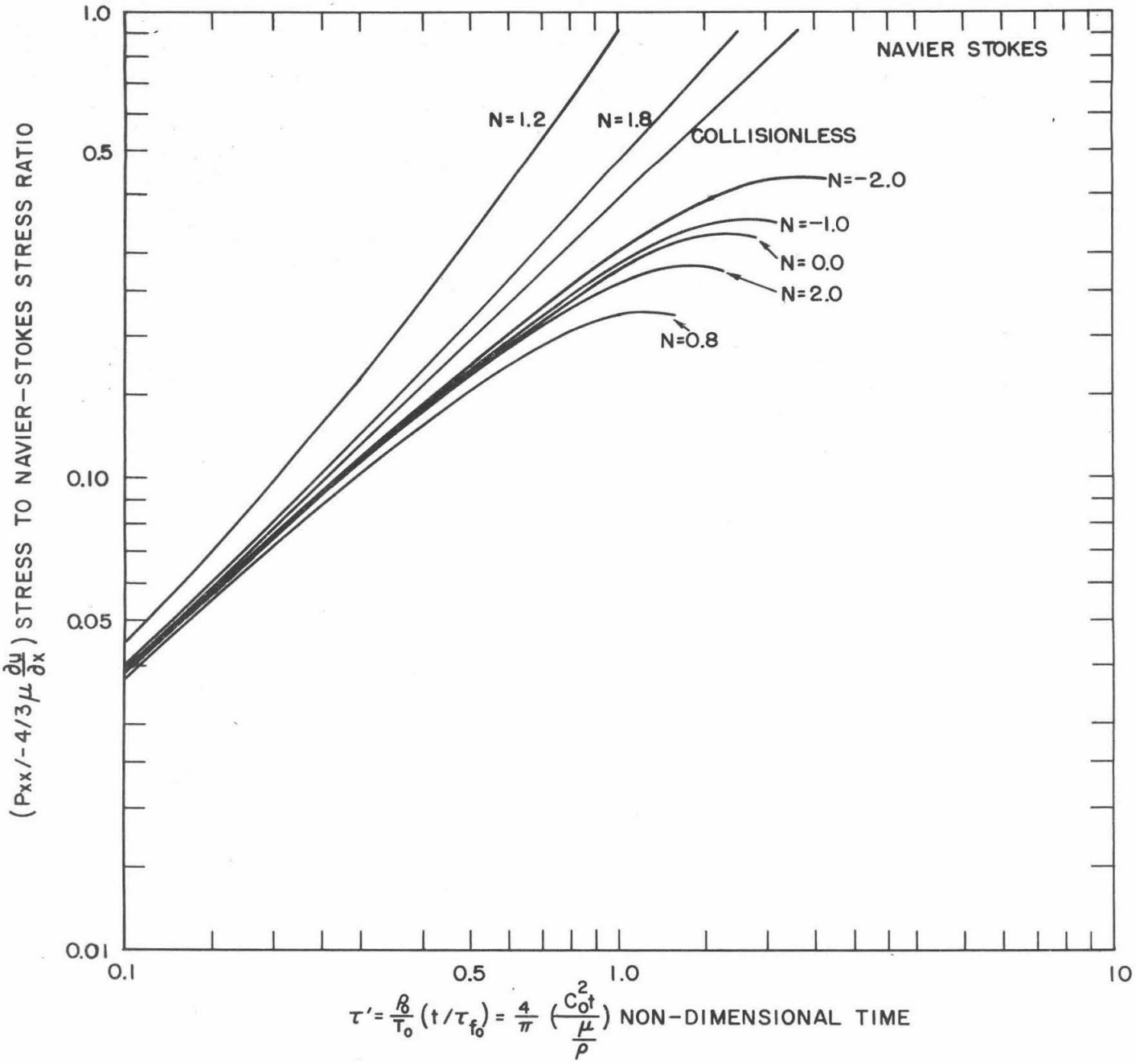

FIG. 18 – STRESS–STRAIN RATE RATIO VS. NORMALIZED TIME (M_s=2.00, ρ_r=0.201×10^{-1})